ANALYSIS OF FREE TURBULENT SHEAR FLOWS BY NUMERICAL METHODS*

By H. H. Korst, W. L. Chow,
University of Illinois at Urbana-Champaign

R. F. Hurt,
Bradley University

R. A. White, and A. L. Addy
University of Illinois at Urbana-Champaign

SUMMARY

Analysis of free turbulent shear flows inherently requires the utilization of conceptual and quantitative formulations concerning the exchange mechanisms. The effort has essentially been directed to classes of problems where the phenomenologically interpreted effective transport coefficients could be absorbed by, and subsequently extracted from (by comparison with experimental data), appropriate coordinate transformations. The transformed system of differential equations could then be solved without further specifications or assumptions by numerical integration procedures.

An attempt has been made to delineate different regimes for which specific eddy viscosity models can be formulated. In particular, this will account for the carryover of turbulence from attached boundary layers, the transitory adjustment, and the asymptotic behavior of initially disturbed mixing regions. Such models have subsequently been used in seeking solutions for the prescribed two-dimensional test cases yielding apparently a better insight into overall aspects of the exchange mechanisms.

Considerable difficulty has been encountered in the utilization of computer programs dealing with axially symmetric geometry as they presently exist at the University of Illinois at Urbana-Champaign. Consequently, only a brief account of these methods and programs has been included – mainly in the form of references.

INTRODUCTION

Much progress in understanding flow separation, separated flows, and wakes has been made since the mutual dependence between viscid and inviscid flow regions has been properly recognized. Development of an attached boundary layer, its separation from solid boundaries forming a free shear layer capable of mass entrainment

*This work was partially supported by NASA through Research Grant No. NsG-13-59 and subsequently through NGL-14-005-140.

from the wake, and energy transfer to and across individual streamlines have been related to the recompression process at the end of the wake and thus have allowed the analysis of previously not understood flow problems of practical importance.

Over more than a decade, work at the University of Illinois at Urbana-Champaign has been focused on propulsion problems relating to base pressure, base heating, and ejector nozzles for thrust augmentation, and so forth. In support of a comprehensive systems approach (based on the understanding of constituent flow components) much attention had to be given to free shear layers which has resulted in both analytical and experimental programs. These efforts have, however, been clearly guided by, and subordinated to, practical objectives.

When called to the task of participating in the present effort, the authors were restricted, naturally, to what had already been developed for serving their own programs. The response is, therefore, selective inasmuch as some of their computer programs have not been found flexible enough to handle all the cases submitted to the predictors.

SYMBOLS

c	concentration of species
c_p	specific heat at constant pressure
C	Crocco number
d	viscosity index
D	energy defect thickness
f	dimensionless stream function (similarity solution)
g	function of transformed x-coordinate
h	enthalpy
I	integrals defined in reference 6
k	thermal conductivity
L	reference length

M	molecular weight or Mach number
Pr_t	turbulent Prandtl number
r	radius
R	gas constant
Re_x	Reynolds number based on x, $u_a x/\nu_a$
Sc_t	turbulent Schmidt number
T	temperature
u	longitudinal velocity component
v	transverse velocity component
W	dimensionless center-line velocity defect
x	longitudinal coordinate
x_o	shifted origin position
y	transverse coordinate
δ	boundary-layer thickness
δ^{**}	momentum thickness of boundary layer
δ^{***}	energy thickness of boundary layer
ϵ	eddy diffusivity
$\zeta = \frac{r}{r_a}$	where r_a is the radius of the central jet
η	similarity variable
θ	static temperature ratio

Λ	stagnation temperature ratio
μ	dynamic viscosity
ν	laminar kinematic viscosity
ξ	dimensionless x-coordinate
$\overline{\xi}$	transformed coordinate
ρ	density
σ	spread rate parameter
σ_o	spread rate parameter for incompressible flow
ϕ	dimensionless velocity
ψ	stream function
$\overline{\psi}$	dimensionless stream function

Subscripts:

a	faster free stream
asy	asymptotic condition
b	slower free stream
c	center-line value
d	particular viscosity index value, or the dividing streamline
e	error function
ℓ	laminar state
o	stagnation state

RA large value of η

t turbulent or transitional state

1,2,4 integrals in reference 6

ANALYSIS

This analysis is restricted at the outset to constant-pressure mixing. Any additional assumptions, as they will affect the mathematical rigor or impose physical restrictions on the solution, will be discussed as they are introduced.

It will be useful to differentiate between kinematic and dynamic similarity when single-independent-variable solutions are utilized. The former refers to nonasymptotic mixing profiles which can be related to similarity profiles by accounting for initial disturbances through appropriate coordinate shifts. Normally, such profiles will not exhibit dynamic similarity as the initial exchange mechanism is not consistent with that of the "matched" solution. On the other hand, when the initial profile of the mixing region results from a strong expansion of an attached boundary layer, there may be nearly dynamic similarity within a newly started shear region at the very edge of the expanded profile, while the growth of the dissipative shear regions occurs within a vortex layer and thus does not exhibit kinematic similarity.

TWO-DIMENSIONAL MIXING

Fundamental Equations

The conservation equations for a pure substance[1] are

$$\frac{\partial}{\partial x}(\rho u) + \frac{\partial}{\partial y}(\rho v) = 0 \tag{1}$$

$$\rho u \frac{\partial u}{\partial x} + \rho v \frac{\partial u}{\partial y} = \frac{\partial}{\partial y}\left(\epsilon_t \rho \frac{\partial u}{\partial y}\right) \tag{2}$$

$$\rho u c_p \frac{\partial T}{\partial x} + \rho v c_p \frac{\partial T}{\partial y} = \frac{\partial}{\partial y}\left(k_t \frac{\partial T}{\partial y}\right) + \rho \epsilon_t \left(\frac{\partial u}{\partial y}\right)^2 \tag{3}$$

The stream function is now introduced

$$\frac{\partial \psi}{\partial y} = + \frac{\rho}{\rho_a} u \qquad \frac{\partial \psi}{\partial x} = - \frac{\rho}{\rho_a} v$$

[1] An extension for gas mixtures is discussed subsequently. For a more detailed account, see Hurt (ref. 1).

and new dimensionless variables defined

$$\phi = \frac{u}{u_a} \qquad \xi = \frac{x}{L} \qquad \overline{\psi} = \frac{\psi}{u_a L} \qquad \theta = \frac{T}{T_a} = \frac{\rho_a}{\rho} \tag{4}$$

where $\overline{\psi}$, related to the stream function ψ, is to be used as an independent variable in the Von Mises plane. Accordingly, after introducing the free-stream Crocco number,

$$C_a{}^2 = \frac{u_a{}^2}{2c_p T_{o_a}} \tag{5}$$

and accounting for the transport mechanisms by the kinematic viscosity $\epsilon_t = \frac{\mu_t}{\rho}$ and the effective Prandtl number Pr_t, the following equations are obtained:

$$\left.\frac{\partial \phi}{\partial \xi}\right|_{\overline{\psi}} = \frac{\partial}{\partial \overline{\psi}}\left|_{\xi}\left[\frac{\epsilon_t}{Lu_a}\frac{\phi}{\theta^2}\left.\frac{\partial \phi}{\partial \overline{\psi}}\right|_{\xi}\right]\right. \tag{6}$$

$$\left.\frac{\partial \theta}{\partial \xi}\right|_{\overline{\psi}} = \frac{\partial}{\partial \overline{\psi}}\left[\frac{1}{Pr_t}\frac{\epsilon_t}{Lu_a}\frac{\phi}{\theta^2}\left.\frac{\partial \theta}{\partial \overline{\psi}}\right|_{\xi}\right] + \frac{\epsilon_t}{Lu_a}\frac{2C_a{}^2}{1 - C_a{}^2}\frac{\phi}{\theta^2}\left(\frac{\partial \phi}{\partial \overline{\psi}}\right)^2 \tag{7}$$

A far reaching simplification of the analysis can be achieved by setting (ref. 2)

$$\mu_t \rho^{(1-d)} = f(\xi) \tag{8}$$

where $d = 1 - \omega$ (ω being the exponent of the Sutherland equation for the dynamic viscosity of a gas) corresponds to the laminar mixing problem.

The transformation

$$d\overline{\xi} = \frac{1}{Re_L}\frac{\epsilon_t}{\nu_\ell \theta^{2-d}}\, d\xi \tag{9}$$

then produces a pair of parabolic simultaneous partial differential equations which can be solved without reference to any specific assumption concerning exchange mechanisms (except d and Pr_t). These equations are

$$\frac{\partial \phi}{\partial \overline{\xi}} = \frac{\partial}{\partial \overline{\psi}}\left(\frac{\phi}{\theta^d}\frac{\partial \phi}{\partial \overline{\psi}}\right) \tag{10}$$

$$\frac{\partial \theta}{\partial \overline{\xi}} = \frac{1}{Pr_t}\frac{\partial}{\partial \overline{\psi}}\left(\frac{\phi}{\theta^d}\frac{\partial \theta}{\partial \overline{\psi}}\right) + \frac{2C_a{}^2}{1 - C_a{}^2}\frac{\phi}{\theta^d}\left(\frac{\partial \phi}{\partial \overline{\psi}}\right)^2 \tag{11}$$

For given initial conditions, step-by-step integrations using implicit iterative procedures for better convergence (see ref. 3) can be carried out with the help of high-speed digital computers.

Results appear in the form of $\phi\left(\bar{\xi},\bar{\psi}\right)$ and $\theta\left(\bar{\xi},\bar{\psi}\right)$ and the coordinate y/L is found from

$$\psi = \int_0^{y/L} \frac{\phi}{\theta}\, d\left(\frac{y}{L}\right) \tag{12}$$

Similarity Solutions

"Exact solutions".- By starting with equation (10) and following the development for nonisoenergetic mixing of two uniform streams having identical compositions (ref. 4), an effective Prandtl number of unity, and satisfying the boundary conditions

$$y \to -\infty, \quad u \to u_b, \quad T_o \to T_{o_b}$$

$$y \to +\infty, \quad u \to u_a, \quad T_o \to T_{o_a}$$

leads to

$$f''' + \left[\frac{\Lambda - C_a{}^2 f'^2}{1 - C_a{}^2}\right]^d ff'' - d\left(\Lambda' - 2C_a{}^2 f' f''\right)\frac{f''}{\Lambda - C_a{}^2 f'^2} = 0 \tag{13}$$

where $f(\eta) = \dfrac{\bar{\psi}}{g\left(\bar{\xi}\right)}$, $f'(\eta) = \phi$, η is the independent similarity variable defined by

$$\left.\frac{\partial \eta}{\partial \bar{\xi}}\right|_{\bar{\psi}} = -\frac{fg'}{f'g} \tag{14}$$

$$\left.\frac{\partial \eta}{\partial \bar{\psi}}\right|_{\bar{\xi}} = \frac{1}{gf'} \tag{15}$$

and primes indicate differentiation with respect to the respective independent variable. From the assumption of similarity, it follows that one may set

$$gg' = 1$$

so that

$$g\left(\bar{\xi}\right) = \sqrt{2\bar{\xi}} \tag{16}$$

and the transformation to physical coordinates can be accomplished with

$$\int \theta \, d\eta = \int \frac{1}{\sqrt{2\xi}} d\left(\frac{y}{L}\right) \tag{17}$$

By adopting Göertler's formulation (ref. 5) of σ,

$$\frac{\epsilon_t}{\nu\theta^{2-d}} = \frac{1}{4\sigma_d{}^2} Re_L \frac{x}{L} \tag{18}$$

one obtains

$$2\sigma_d \frac{y}{x} = \int_{\eta_j}^{\eta} \theta \, d\eta \tag{19}$$

where the origin of y is placed at the zero streamline where $f(\eta_j) = 0$. The notation σ_d has been introduced to stress the fact that the similarity parameter σ depends not only on the procedure of matching between an experimental and an analytical profile but also on the choice (if one is needed or indicated) of the analytical formulation (ref. 4).

An extension to analyze the mixing of two streams having different gas constants R_a and R_b is easily accomplished for Prandtl and Lewis numbers of unity by the expression

$$\frac{\rho_a}{\rho} = \frac{1}{1 - C_a{}^2} \left\{ \frac{\left[\phi\left(1 - \frac{R_b}{R_a}\right) + \frac{R_b}{R_a} - \phi_b\right]\left[\phi - \phi_b + \frac{T_{o_b}}{T_{o_a}}(1 - \phi)\right]}{(1 - \phi_b)^2} - \phi^2 C_a{}^2 \right\} \tag{20}$$

(See discussion of test case 3, also.)

Error function solution.- Proposed as a first-order approximation for solving equation (10) under the conditions of incompressible flow with $d = 0$ by Göertler (ref. 5), the error function distribution for the velocity profile is

$$\phi = \frac{1}{2}(1 + \phi_b) + \frac{1 - \phi_b}{2} \operatorname{erf} \eta \tag{21}$$

where $\eta = \sigma_e\left(\frac{y}{x}\right)$. The error function solution has been widely used for momentum integral methods devised to deal with compressible, diabatic (ref. 6), and even reactive (ref. 7) free shear layers. Auxiliary integrals for determining mass, momentum, and energy transfer, as well as shear stress, dissipation rates, and property distributions, have been tabulated (ref. 6) or made subroutines of more comprehensive programs dealing with propulsion problems (ref. 8). A discussion of differences between spread rate parameters $(\sigma_e, \sigma_d, \text{etc.})$ has been included in reference 4.

Initially Disturbed Mixing Region

Similarity solutions are reached asymptotically as the influence of initial disturbances (in velocity and property profiles and in the exchange mechanism) decreases. The gradual approach to similarity profiles can be represented in its latest stages by a lateral shift of mixing profiles, that is, by satisfying the momentum integrals. This still leaves open the question of how to interpret properly similarity parameters such as σ when the exchange mechanism is to be evaluated at other than far-downstream locations. Attention will be given to the latter problem in the section on "Eddy Viscosity Concepts."

Origin-shift methods.- Utilization of similarity solutions for initially disturbed profiles by origin-shift methods has been suggested in different forms by various authors, and the work of Hill and Page (ref. 9) and Kessler (ref. 10) may be consulted for further details. Use of the momentum integral for determining lateral and longitudinal coordinate shifts will, however, become unfeasible when wakes or mixing between streams of nearly equal velocity in the presence of relatively large initial disturbances have to be considered. It should be noted that virtual origins for exchange coefficient growth have been found useful in connection with eddy viscosity models employed in finite-difference integrations of the fundamental equations (see the section "Eddy Viscosity Concepts").

Local similarity.- The restriction on the type of viscosity models consistent with the longitudinal coordinate transformation expressed by equation (9) will be found most unrealistic for cases where a relatively thick boundary layer undergoes a rapid expansion (such as in base flows) before the onset of constant-pressure mixing. This can lead to effective quenching of the turbulence level in the expanded profile (which is then rotational but not strongly dissipative) while the dissipative exchange mechanism remains confined to a much narrower shear region (refs. 11 and 12). This shear region exhibits features of local similarity and is initially laminar before undergoing transition. Growth of such transitional shear regions, for single-stream mixing, has been analyzed in some detail by Gerhart (ref. 13), and there seems to be confirmation that the similarity parameter σ retains its qualitative relevance and quantitative value. Since turbulent mixing now appears to originate well downstream of the "expansion corner," agreement with origin-shift methods concerning the energy levels of the dividing streamline is surprising but can be supported by detailed calculations.

Numerical integrations.- Computer programs have been developed to perform the step-by-step numerical integration of the system of equations (refs. 1 and 2), and an implicit iterative method of integration is utilized which improves the economy of the calculations while retaining accuracy and assuring numerical stability.

The integration uses initial and boundary conditions given in physical coordinates x and y but proceeds with calculations in the transformed $\bar{\xi}\bar{\psi}$-plane. Dimensionless velocity $\left(\phi = \frac{u}{u_a}\right)$, temperature $\left(\theta = \frac{T}{T_a}\right)$, or density $\left(\rho/\rho_a\right)$ distributions are then found as

functions of $\bar{\psi}$ (or y/L) for parametric values of the variable $\bar{\xi}$. Location of the $\bar{\xi}$ value with the x-scale depends upon the viscosity law as contained in the transforming equation (eq. (9)) which can be written

$$\bar{\xi} = \frac{1}{Re_L} \int \frac{\epsilon}{\nu_\ell \theta^{2-d}} d\,\frac{x}{L}$$

Attempts have been made to gain information on the integrand by matching of calculated and experimentally determined profiles, for example, by the dissipation integral (ref. 2) or other unique features (such as minimum velocity in wakes). (See section concerned with determination of the eddy viscosity.)

For the problems at hand, however, one needs this information as input, and certain speculative assumptions on the behavior of the turbulent eddy viscosity still are to be specified in the section "Eddy Viscosity Concepts" in order to explain their use for obtaining solutions to the test cases.

AXIALLY SYMMETRIC MIXING REGIONS

An extension of the theoretical analysis and the resulting computer program for jet mixing dealing with axisymmetric geometries and nonhomogeneous gases has been made by Hurt (ref. 1). Like many others (e.g., refs. 14 and 15), he utilizes the system of global conservation equations as well as conservation of species without chemical reactions. The simplifying assumptions are consistent with boundary-layer approximations but, in addition, he assumes a turbulent Lewis number of unity which implies that the turbulent Schmidt and Prandtl numbers are equal to each other yet not necessarily equal to unity individually. Also, specific heats at constant pressures are assumed to be functions of concentrations but not of temperature, which limits his analysis to moderate temperature variations even though it attempts to cope with compressibility. In this sense, and with regard to improved numerical integration procedures, Hurt's work is an extension of that by Donovan and Todd (ref. 15). The resulting set of equations is in analogy with those of the preceding sections except for the accounting for species and the use of a dimensionless enthalpy rather than temperature in the energy equations:

$$\left.\begin{aligned}
\frac{\partial \phi}{\partial \xi} &= \frac{\partial}{\partial \bar{\psi}}\left[\bar{\epsilon}\bar{\rho}^2\zeta^2\phi\,\frac{\partial \phi}{\partial \bar{\psi}}\right] \\
\frac{\partial c_i}{\partial \xi} &= \frac{\partial}{\partial \bar{\psi}}\left[\frac{\bar{\epsilon}}{Sc_t}\,\bar{\rho}^2\zeta^2\phi\,\frac{\partial c_i}{\partial \bar{\psi}}\right]_{i=1,N} \\
\frac{\partial \bar{h}}{\partial \xi} &= \frac{\partial}{\partial \bar{\psi}}\left[\frac{\bar{\epsilon}}{Pr_t}\,\bar{\rho}^2\zeta\phi\,\frac{\partial \bar{h}}{\partial \bar{\psi}}\right] + \frac{2Ca^2}{1 - Ca^2}\,\bar{\epsilon}\bar{\rho}^2\zeta^2\phi\left(\frac{\partial \phi}{\partial \bar{\psi}}\right)^2
\end{aligned}\right\} \qquad (22)$$

Here,

$$\bar{\rho}\frac{u}{u_a} = \frac{1}{\zeta}\frac{\partial\bar{\psi}}{\partial\zeta} \qquad \bar{\rho}\frac{v}{u_a} = -\frac{1}{\zeta}\frac{\partial\bar{\psi}}{\partial\xi}$$

C_a is the Crocco number of the internal stream, and $\bar{\epsilon} = \frac{\epsilon}{u_a r_a}$ were r_a is a reference radius of the coaxial stream, $\bar{\rho} = \frac{\rho}{\rho_a}$, and $\bar{h} = \frac{h}{h_a}$.

In addition, the perfect gas law for isobaric mixing of a multispecies mixture

$$\bar{\rho} = \frac{1}{\gamma\bar{T}} \tag{23}$$

was utilized, where

$$\gamma = \frac{\sum_{i=1}^{N} \frac{c_i}{\bar{M}_i}}{\sum_{i=1}^{N} \frac{c_{a_i}}{\bar{M}_i}} \tag{24}$$

$\bar{M}_i$ is the molecular weight of the ith species, and $\bar{T} = \frac{T}{T_a}$. The static temperature ratio $\bar{T}$ was evaluated from the energy equation and then the stagnation temperature ratio was found by using the following formulation developed from the relationship between stagnation and static enthalpy:

$$\Lambda = \bar{T}\left(1 - C_a{}^2\right) + \left(\frac{\phi^2 C_a{}^2}{\alpha}\right) \tag{25}$$

where

$$\alpha = \frac{\sum_{i=1}^{N} c_i c_{p_i}}{\sum_{i=1}^{N} c_{a_i} c_{p_{a_i}}} \tag{26}$$

and Λ is the local stagnation temperature ratio. In contrast to the two-dimensional case, the transformation of the streamwise coordinate ξ (to eliminate the eddy viscosity from the equation) was not included in Hurt's analysis. This was due to evidence that the effective turbulent exchange coefficient could not be considered, with sufficient accuracy, to be a function of the streamwise coordinate only. His program, thus, can accommodate as input suitable eddy viscosity models. At this stage, however, there do not appear to be

sufficient experimental data and insight into controlling mechanisms to expect a simple yet universal formulation for a phenomenological eddy viscosity model.

It is of interest to note the efforts of Spalding and his coworkers at Imperial College (e.g., ref. 16) and others to gain a better insight into turbulent exchange mechanisms by use of multiparameter models involving the kinetic energy of turbulent motion.

EDDY VISCOSITY CONCEPTS

Within the restrictions imposed by the coordinate transformation (eq. (9)) and the resulting coupling of the viscosity to the density for two-dimensional mixing problems, there is still the possibility of coping with fully laminar, fully turbulent, and transitional cases. The initial conditions have first to be examined.

INITIAL CONDITIONS RELATED TO APPROACHING BOUNDARY LAYER

A mixing region can be the result of flow separation associated with

(i) Constant pressure (wake behind a flat plate)

(ii) An acceleration (as in the supersonic base pressure problem)

(iii) A pressure rise (due to an adverse pressure gradient)

In any one of these cases, the attached boundary layer will cause an initial disturbance for the mixing region. Each case, however, will be different in its kinematic and dynamic effects.

The constant-pressure case appears to be the simplest. One would expect that both the flow profile and the viscous structure remain virtually unchanged. The acceleration causes a change in the velocity profile (which could possibly be accounted for by a streamline expansion method), but it also tends to quench the turbulent mechanism (refs. 11 and 12). This can lead to the situation discussed in the section "Local Similarity" which produces a transitional problem in a "mixing sublayer" imbedded in a vortex layer.

Separation associated with a pressure rise presents the most complicated problem and points to the need for a momentum integral approach (ref. 17) and origin-shift treatment of the mixing zone (e.g., ref. 10).

INITIAL EXCHANGE MECHANISMS

It is evident that a mere description of velocity, temperature, and concentration profiles will, in the turbulent case, generally not be sufficient to solve the problem of computing the development of the mixing region. What is missing could be most important – at

least for the early stages of the mixing process – namely, its initial mechanisms. Only case (i) does provide such information if one uses the work of Maise and McDonald (ref. 18). Case (ii), on the other hand, generates local similarity – provided the expansion is sufficiently "strong" – first in the laminar (or "laminarized") mixing sublayer and then in its turbulent continuation where one depends on information on transition Reynolds numbers, such as given by Chapman, Kuehn, and Larson (ref. 19). Case (iii), because of its complexity, raises special interest for exploring how quickly initial conditions become submerged in the mechanisms generated by the mixing process itself. In the next section a tentative model for developing turbulent shear layers is projected.

FULLY TURBULENT MIXING BETWEEN TWO STREAMS ORIGINALLY SEPARATED BY A FLAT PLATE

As each stream approaches the trailing edge of the plate, it possesses its individual boundary layers having thickness, momentum thickness, and energy thickness, the corresponding shape factors, and an eddy viscosity distribution as given by Maise and McDonald (ref. 18) or determined with more precision by extensions of their method (e.g., to account for heat transfer).

Initial Level of Eddy Viscosity

If conditions in the two streams are very dissimilar, the eddy viscosity level in one of them may be dominating at the point of confluence. As the restraint on fluctuations imposed by the wall is removed, it seems logical to assume that the peak value of the eddy viscosity will originally prevail. It is of interest to note that such peak values can be correlated, for a wide range of Mach numbers, by the simple relation

$$\left.\frac{\epsilon_t}{\nu}\right|_{peak} = \frac{Re_\delta^{0.896}}{120} \tag{27}$$

Filling of the Wake

Breakup of the laminar sublayer and the large velocity gradient generated in the attached boundary layer control the next phase. If this process can be considered (at least for that portion of the profile where the mixing mechanism is most effective) to be reasonably close to the asymptotic single-stream jet mixing condition,

$$\frac{\epsilon}{\nu} = \frac{1}{4\sigma^2} Re_L \frac{x}{L} \tag{28}$$

may be selected where σ is related to the flow conditions in the faster stream, and the origin for x is at the point of confluence. (This scheme is akin to the concept of local similarity.)

Approaching the Asymptotic Solution

With the jet mixing mechanism thus building up, it will eventually approach the asymptotic case for both the kinematic and dynamic aspects.

At the matching conditions, after selecting an appropriate similarity profile, one has to account for both the momentum and energy defects at $x = 0$.

This can be achieved by applying an origin shift x_o and by utilizing the concept of equivalent bleed (ref. 6). By using the integrals defined and tabulated in reference 6 for the error function profile, one relates the mechanical energy defect in the approaching streams at $x = 0$, $D = \dfrac{\delta_a^{***} + \phi_b^3 \delta_b^{***}}{2}$ through

$$\frac{2\sigma D}{(-x_o) u_a^3 \rho_a} = \left[I_1(\eta_{RA}) - I_1(\eta_d)\right](1 - \phi_b^2) - I_4(\eta_{RA}) \tag{29}$$

while the momentum defect is accommodated through the concept of equivalent bleed which determines

$$I_1(\eta_d) = \frac{1}{1 - \phi_b}\left[I_1(\eta_{RA}) - I_2(\eta_{RA}) - \sigma(\Delta a + \Delta b)\right] \tag{30}$$

where

$$\Delta a = \frac{\delta_a^{**}}{(-x_o)}$$

$$\Delta b = \frac{\rho_b}{\rho_a} \phi_b^2 \frac{\delta_b^{**}}{(-x_o)}$$

and

$$\phi_b \neq 1$$

Combining equations (29) and (30) yields, for the origin shift,

$$x_o = \sigma \frac{(1 + \phi_b)\left[\delta_a^{**} + \dfrac{\rho_b}{\rho_a} \phi_b^2 \delta_b^{**}\right] - \left(\delta_a^{***} + \phi_b^3 \delta_b^{***}\right)}{I_1(\eta_{RA})(1 - \phi_b^2) - I_4(\eta_{RA}) - (1 + \phi_b)\left[I_1(\eta_{RA}) - I_2(\eta_{RA})\right]} \tag{31}$$

The similarity parameter σ refers here to the two-stream case (ref. 6).

It is necessary to comment on the manner in which the asymptotic case is "approached." If the "filling of the wake" (in the sense of the preceding section) becomes pronounced due to $\phi_b > 0$, the increase in eddy viscosity described by equation (28) will initially prevail over that related to the asymptotic solution. Hence, an overshoot will be

experienced so that the approach to the asymptotic profile occurs in the sense of relaxation rather than amplification of the mixing mechanism.

For the case where $\phi_b = 0$, such an overshoot should be less pronounced. The energy defect integral, as utilized for determining the origin shift x_o, differs from the dissipation integrals defined in reference 2)

$$DI = \int_{-\infty}^{+\infty} \frac{\phi}{\theta}(1 - \phi)\left(\phi - \phi_b\right)\frac{dy}{L} \tag{32}$$

or

$$DI = \int_{-\infty}^{+\infty} (1 - \phi)\left(\phi - \phi_b\right)d\overline{\psi} \tag{33}$$

only by a constant value (due to the fact that the momentum of the mixing streams is preserved once external forces such as wall shear friction are not present). The dissipation integral has been evaluated and presented in graphical form as shown in figure 1 for a variety of flow conditions.

Use of both forms (eq. (32) for the experimental profile and eq. (33) for the analytical solution) is then convenient for establishing the relation between x/L and $\overline{\xi}$ and $\epsilon/\nu(x/L)$.

Wake Problem – Both Streams Having Identical Velocities and Initial Boundary Layers

For wake flows, the asymptotic solution shall be represented by a constant level of the eddy viscosity (Schlichting (ref. 5)) so that, with reference to the momentum thickness of one approaching boundary layer,

$$\frac{\epsilon}{\nu} = 0.0888 Re_L \frac{\delta_a^{**}}{L} \tag{34}$$

Proposed Models for Turbulent Eddy Diffusivity

A schematic presentation of eddy viscosity models as used in the present study is shown in figure 2.

RELATION BETWEEN THE STREAMWISE COORDINATES x AND $\overline{\xi}$

The proposed eddy viscosity model establishes a relation between the transformed coordinate $\overline{\xi}$ and the physical coordinate x, and thus allows identification and location of the calculated mixing profiles

$$\bar{\xi} = \int \frac{\epsilon}{\nu_\theta^{2-d}} \frac{1}{Re_L} d\left(\frac{x}{L}\right) + \text{Constant} \tag{35}$$

DETERMINATION OF THE EDDY VISCOSITY FROM MATCHING OF EXPERIMENTAL AND ANALYTICAL PROFILES

The concepts developed for ϵ/ν in the preceding sections are essentially conjectures. Indeed, the analytical model and the calculation procedures have been worked out in such a way as to remove the need for depending on a specific viscosity law. Actually, one can utilize equation (9) for determining the viscosity law.

To accomplish this, it is necessary to define the matching of profiles for value pairs of x and $\bar{\xi}$, which leads to a unique $\bar{\xi} = \bar{\xi}(x)$ relationship which then can yield, for $d = 2$

$$\frac{\epsilon}{\nu} = \left.\frac{d\bar{\xi}}{d\left(\frac{x}{L}\right)}\right|_x Re_L \tag{36}$$

Obviously, only single parameters can be matched for both the calculated and the experimental profiles.

Two possible choices are

(i) The minimum velocity, as it is well defined in wake problems

(ii) The dissipation integral given by equations (29), (32), and (33)

An illustration of this procedure is given in the section "Test Case – Solutions."

EDDY VISCOSITY IN AXIALLY SYMMETRIC MIXING REGIONS

Much uncertainty exists concerning suitable turbulent exchange coefficient formulations for axially symmetric flow. The appearance of the transverse coordinate r in the conservation equations also complicates the situation since it would restrict the possibilities of a transformation (e.g., eq. (9) for the two-dimensional case) to the unattractive form where a singularity in the exchange coefficient could occur as $r \to 0$. Empirical relations, therefore, still are favored in dealing with individual cases (ref. 1) but apparently cannot be expected to give satisfactory results when applied to widely different flow conditions. (See discussion of test case 11.)

TEST CASE – SOLUTIONS[2]

TEST CASE 1: TWO-DIMENSIONAL SHEAR LAYER

Spreading Parameter for a Fully Developed Incompressible Free Shear Layer (Influence of ϕ_b)

The effect of the free-stream velocity ratio $\frac{u_b}{u_a} = \phi_b$ on the spreading parameter σ for similarity mixing profiles has recently been reviewed by Yule (ref. 20). Shown in figure 3 is the relation

$$\frac{\sigma_o}{\sigma} = \frac{1 - \phi_b}{1 + \phi_b}$$

as presently used in computer programs at the University of Illinois and which also has been utilized for calculations of asymptotic mixing regions in the discussion of test case 4.

TEST CASE 2: TWO-DIMENSIONAL SHEAR LAYER

Spreading Parameters for a Fully Developed Turbulent Free Shear Layer With Zero Velocity Ratio (Influence of Mach Number)

Much uncertainty exists as to the effects of Mach number on the mixing mechanism, as can be illustrated by the large discrepancies for observed or predicted values for σ (ref. 9). Shown in figure 4 is the simple linear relationship

$$\sigma = 12 + 2.76M_a$$

as proposed for use in the lower Mach number range $M_a < 3$ (ref. 6).

TEST CASE 3: TWO-DIMENSIONAL SHEAR LAYER

Spreading Parameter for a Fully Developed Low-Speed Free Shear Layer With a Velocity Ratio of 0.2 and Density ratios ρ_b/ρ_a of 14, 1/2, 1/7, and 1/14

It is the judgment of the authors that conclusions concerning spread parameters must be based on more extensive and reliable experimental data than appears to be presently available. Evaluation of earlier experiments by Pabst (ref. 21) conducted for a single temperature ratio of 2.3 did not show an appreciable effect on σ. To facilitate future correlations, theoretical calculations for $\sigma_d(\Delta y/x)$ based on the procedure outlined in the section "Similarity Solutions" with a selected value for $d = 2$ are presented in figure 5. The abscissa in figure 5 represents either the ratio of T_b/T_a or ρ_a/ρ_b since

[2] $d = 2$ for all calculations presented.

low-speed flows are being considered. According to equation (20), the effects of the stagnation temperature ratio and gas constant ratio should be equivalent.

TEST CASE 4: TWO-DIMENSIONAL SHEAR LAYER

Influence of Initial Boundary Layers, Incompressible Flow, $\phi_b = 0.35$

As requested, results of theoretical calculations for the velocity profiles are shown in figure 6. The corresponding shear stress distributions are given in figure 7. The correlation procedure between the physical and transformed dimensionless streamwise coordinates x/L and $\bar{\xi}$ is illustrated by the use of the dissipation integrals according to equations (32) and (33) in figures 8 and 9. The extracted information on the effective turbulent eddy viscosity ϵ/ν is shown in figure 10.

This figure also compares these viscosity coefficients with those resulting from the concepts developed in the section "Eddy Viscosity Concepts." A strong overshoot as a continuation of the wake-filling mechanism over the asymptotic solution is clearly evidenced.

TEST CASE 5: TWO-DIMENSIONAL SHEAR LAYER

Initial Development of a Turbulent Compressible Free Shear Layer

The requested theoretically calculated velocity profiles are shown in figure 11. One must note that the y-scale in figure 11 reflects conservation of momentum, while the experimental data require a translation to satisfy this physical constraint. Figures 12 and 13 have been added to show the degree of agreement between the eddy viscosity distributions based on the dissipation integral correlation and the concepts proposed in the section "Eddy Viscosity Concepts." Again, an overshoot is noted, but it is rather moderate since no wakelike contribution exists for $\phi_b = 0$.

TEST CASES 6 TO 13, 15, AND 17 TO 23: AXIALLY SYMMETRIC FLOW CASES

Considerable difficulty has been encountered in attempts to obtain numerical computer solutions by using the approach and programs of reference 1. This situation has been caused primarily by communication problems (Dr. Hurt had left the University of Illinois) and by difficulties encountered in switching to a different computer system with limited storage capacity. Consequently, attention is directed to reference 1 as containing specific examples for program capabilities. In addition, calculated center-line velocity distributions as they apply to test case 11 are shown in figure 14.

TEST CASE 14: TWO-DIMENSIONAL WAKE – LOW SPEED

Shown in figure 15 is the center-line velocity development as a function of the transformed coordinate $\bar{\xi}$. Figure 16 illustrates the use of the presently proposed viscosity model for the three regimes described previously. This produces the plot of $1/W^2$ as a function of $x/\delta_a{}^{**}$ (fig. 17), which is the required answer to this test case. Agreement with experimental data was found to be reasonably good.

TEST CASE 16: TWO-DIMENSIONAL WAKE – SUPERSONIC ADIABATIC FLOW

With transition at station 1, the present viscosity model assumes the form shown in figure 18 with experimental ϵ/ν values (obtained with the help of dissipation function correlation) also presented. A strong overshoot along the trough-concept-rise is noticed with subsequent relaxation towards the asymptotic (constant ϵ) solution. It must be noted that the theoretical calculations for $1/W^2$ as a function of x/D (fig. 19 (required)) and T_c/T_a as a function of x (fig. 20) have been obtained by following the trough-rise portion. The difference between the "relaxing" and the "rising" ϵ/ν branch should, however, not produce significant differences, especially in view of the rather large scatter of experimental data. Overshoot and subsequent relaxation of ϵ/ν is experimentally – albeit indirectly – evidenced by figure 1 of reference 22. Computer results $\left(\phi_c \text{ and } T_c/T_a \text{ as a function of } \bar{\xi}\right)$ are presented in figure 21.

TEST CASE 24: TWO-DIMENSIONAL WAKE – COMPRESSIBLE DIABATIC FLOW (TRANSITIONAL)

Prandtl number for this case has been selected as 0.72 throughout. This is consistent with the expectation of a significantly long laminar mixing region followed by transition and turbulent mixing for which $Pr_t = 0.72$ is incidentally a reasonable approximation. Based on theoretical calculations, and with the use of information on transition in free shear layers (ref. 19), one arrives at a transition location of 7.01 cm (2.76 in.) corresponding to $Re_x = 180\,000$ where

$$Re_x = \frac{Re_L\left(x_t/L\right)_t}{\left(T_c/T_a\right)_i^2}$$

The resulting relation between ϵ/ν and x/L is shown in figure 22. Correlation between $\bar{\xi}$ and x/L by the integration of equation (9) and the finite-difference calculations $\left(\phi_c,\ T_c/T_a \text{ as a function of } \bar{\xi} \text{ in fig. 23}\right)$ then produce figure 24 which shows

$1/W^2$ as a function of x/D and figure 25 which is a comparison of calculated and measured center-line temperature ratios. It is of interest to note the effects of transition as they appear in both the calculated and experimentally determined data.

REFERENCES

1. Hurt, Robert Frank: A Theoretical and Experimental Investigation of Axisymmetric, Non-Homogeneous, Compressible Turbulent Mixing. Ph. D. Thesis, Univ. of Illinois at Urbana-Champaign, 1970.

2. Lilienthal, Peter Frederick, II: Development of Viscous Free Shear Layers Between Two Compressible Constant Pressure Isoenergetic Streams With Special Considerations of Its Dissipative Mechanisms. Ph. D. Thesis, Univ. of Illinois, 1970.

3. Grabow, Richard M.: Finite Difference Methods. Laminar Separated Flows, VKI CN 66a, Von Karman Inst. Fluid Dyn., Apr. 1967.

4. Korst, H. H.; and Chow, W. L.: On the Correlation of Analytical and Experimental Free Shear Layer Similarity Profiles by Spread Rate Parameters. Trans. ASME, Ser. D: J. Basic Eng., vol. 93, no. 3, Sept. 1971, pp. 377-382.

5. Schlichting, Hermann (J. Kestin, transl.): Boundary Layer Theory. Fourth ed., McGraw-Hill Book Co., Inc., c.1960.

6. Korst, H. H.; and Chow, W. L.: Non-Isoenergetic Turbulent $(Pr_t = 1)$ Jet Mixing Between Two Compressible Streams at Constant Pressure. NACA CR-419, 1966.

7. Davis, Lorin R.: Experimental and Theoretical Determination of Flow Properties in a Reacting Near Wake. AIAA J., vol. 6, no. 5, May 1968, pp. 843-847.

8. Addy, A. L.: Thrust-Minus-Drag Optimization by Base Bleed and/or Boattailing. J. Spacecraft & Rockets, vol. 7, no. 11, Nov. 1970, pp. 1360-1362.

9. Hill W. G., Jr.; and Page, R. H.: Initial Development of Turbulent, Compressible, Free Shear Layers. Trans. ASME, Ser. D: J. Basic Eng., vol. 91, no. 1, Mar. 1969, pp. 67-73.

10. Kessler, Thomas J.: Two-Stream Mixing With Finite Initial Boundary Layers. AIAA J., vol. 5, no. 2, Feb. 1967, pp. 363-364.

11. Page, R. H.; and Sernas, V.: Apparent Reverse Transition in an Expansion Fan. AIAA J., vol. 8, no. 1, Jan. 1970, pp. 189-190.

12. Korst, H. H.: Dynamics and Thermodynamics of Separated Flows. Review Lecture presented at 1969 International Seminar on Heat and Mass Transfer in Flows With Separated Regions and Measurement Techniques (Herceg-Novi, Yugoslavia), Sept. 1969.

13. Gerhart, P. M.: A Study of the Reattachment of a Turbulent Supersonic Shear Layer With the Closure Condition Provided by a Control Volume Analysis. Ph. D. Thesis, Univ. of Illinois, 1971.

14. Libby, Paul A.: Theoretical Analysis of Turbulent Mixing of Reactive Gases With Application to Supersonic Combustion of Hydrogen. ARS J., vol. 32, no. 3, Mar. 1962, pp. 388-396.

15. Donovan, Leo F.; and Todd, Carroll A.: Computer Program for Calculating Isothermal, Turbulent Jet Mixing of Two Gases. NASA TN D-4378, 1968.

16. Rodi, W.; and Spalding, D. B.: A Two-Parameter Model Turbulence, and Its Application to Free Jets. Wärme-und Stoffüberstragung, vol. 3, no. 2, 1970, pp. 85-95.

17. White, Robert A.: Effect of Sudden Expansions or Compressions on the Turbulent Boundary Layer. AIAA J., vol. 4, no. 12, Dec. 1966, pp. 2232-2234.

18. Maise, George; and McDonald, Henry: Mixing Length and Kinematic Eddy Viscosity in a Compressible Boundary Layer. AIAA J., vol. 6, no. 1, Jan. 1968, pp. 73-80.

19. Chapman, Dean R.; Kuehn, Donald M.; and Larson, Howard K.: Investigation of Separated Flows in Supersonic and Subsonic Streams With Emphasis on the Effect of Transition. NACA Rep. 1356, 1958.

20. Yule, Andrew J.: Spreading of Turbulent Mixing Layers. AIAA J., vol. 10, no. 5, May 1972, pp. 686-687.

21. Szablewski, W.: Turbulente Vermischung ebener Heissluftstrahlen. Ing.-Arch., Bd. XXV, Heft 1, Jan. 1957, pp. 10-25.

22. Demetriades, Anthony: Observations on the Transition Process of Two-Dimensional Supersonic Wakes. AIAA Paper No. 70-793, June-July 1970.

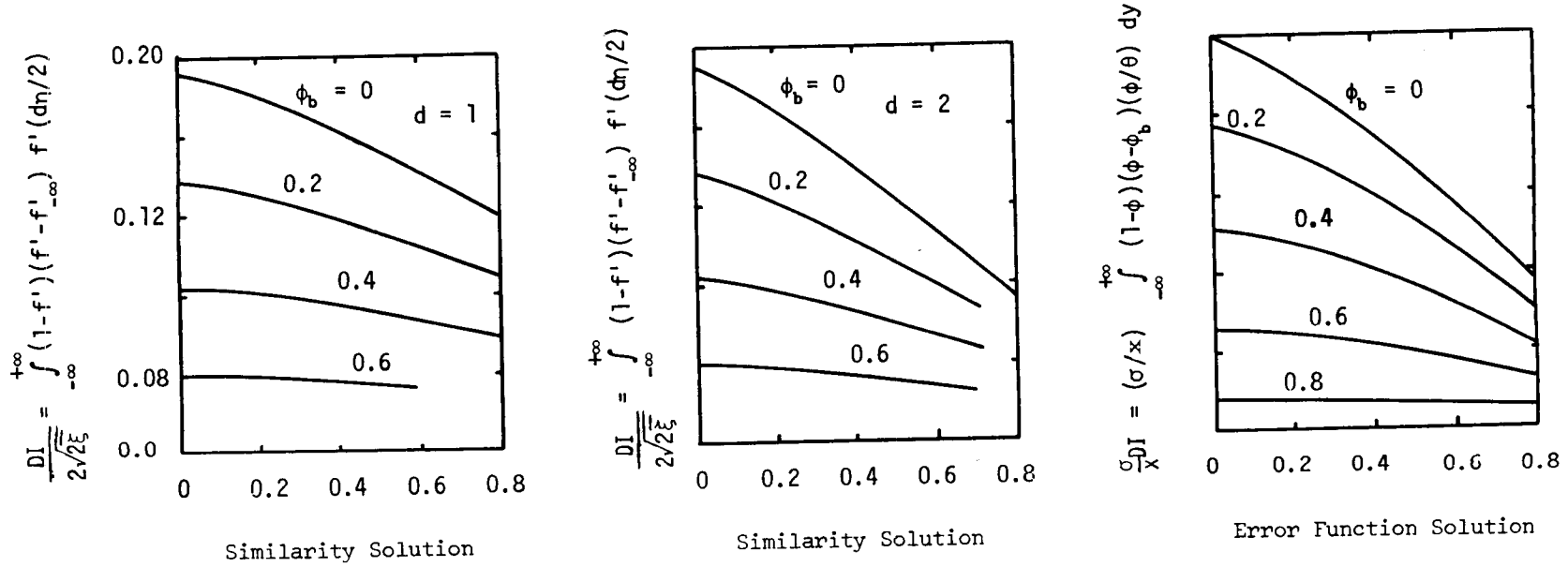

Figure 1.- Total dissipation of mechanical energy as a function of C_a^2 and velocity ratio ϕ_b for $T_{o_a} = T_{o_b}$. (Adapted from ref. 2.)

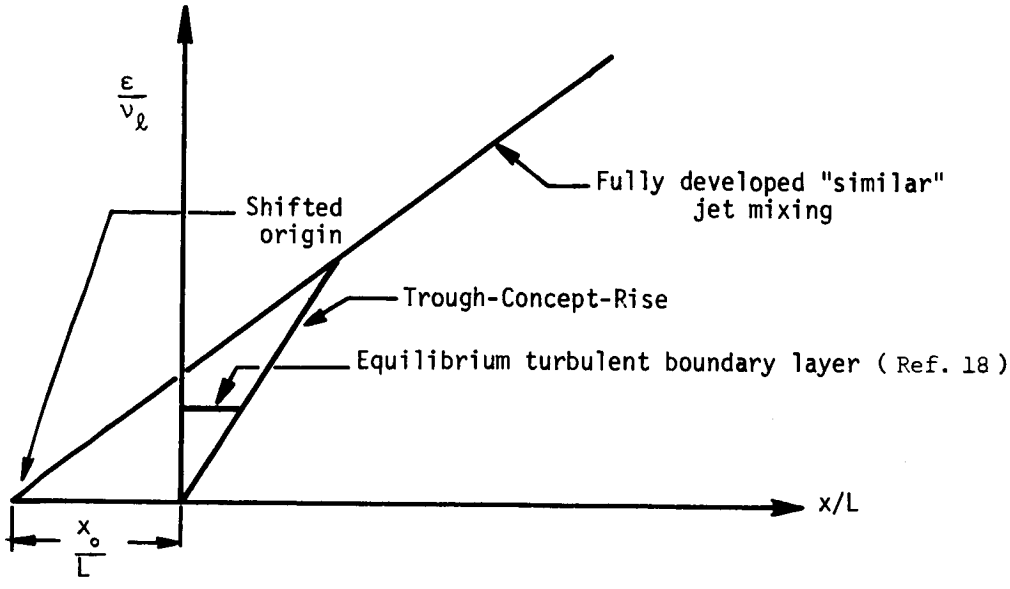

(a) Turbulent free jet mixing.

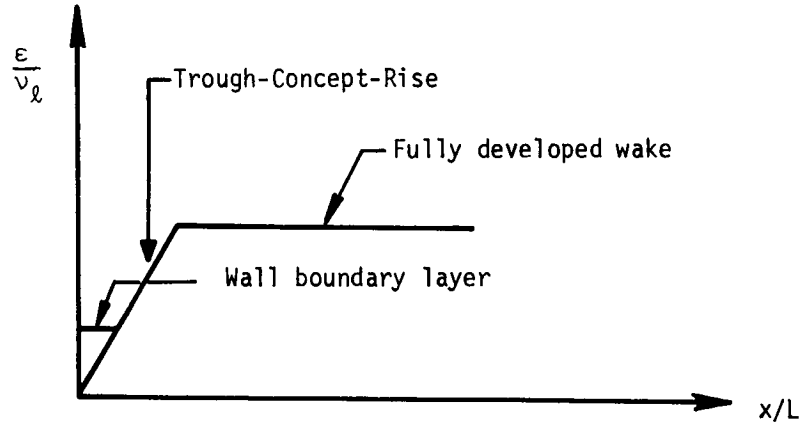

(b) Turbulent wake flow.

Figure 2.- Viscosity model.

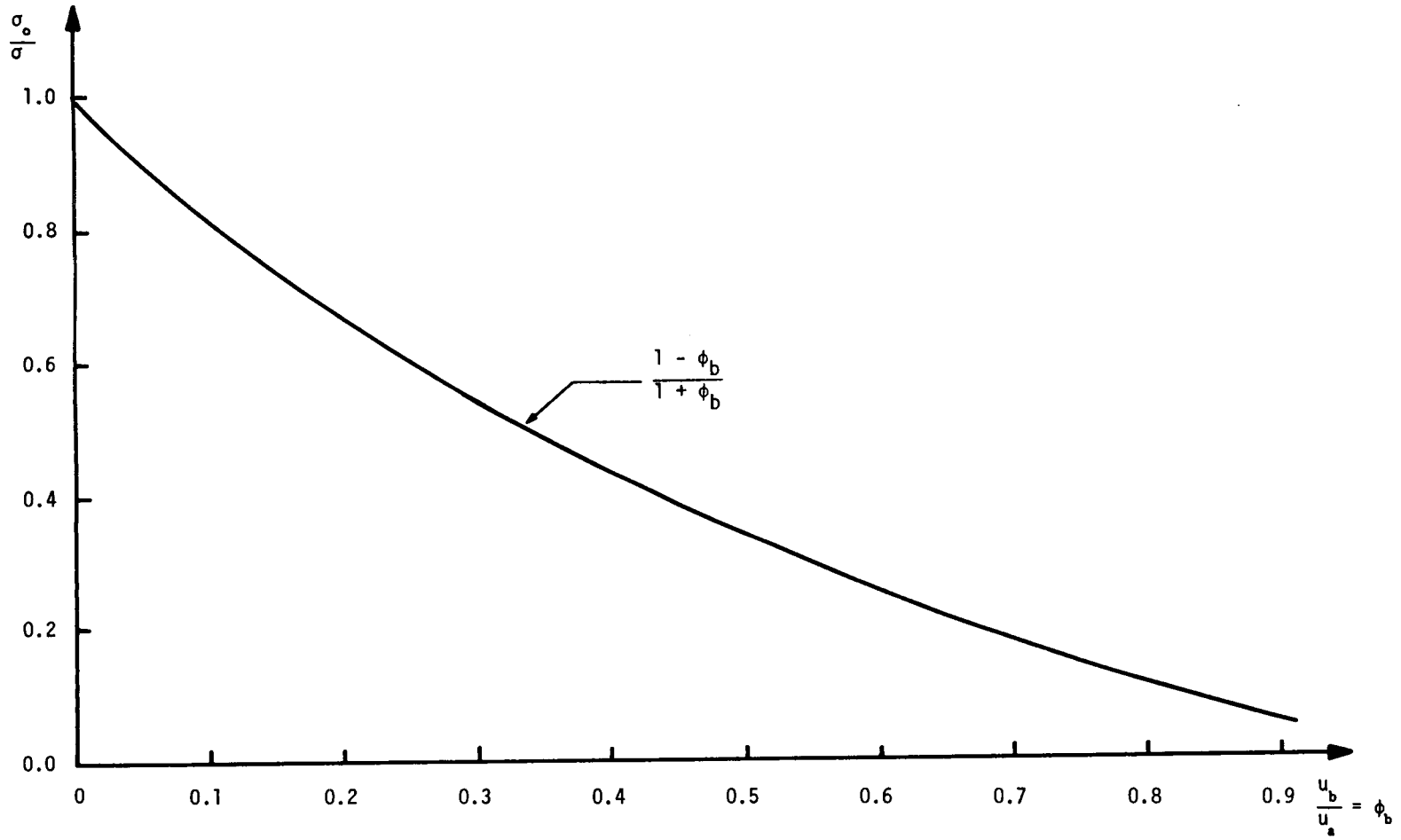

Figure 3.- Influence of velocity ratio ϕ_b on similarity parameter σ.

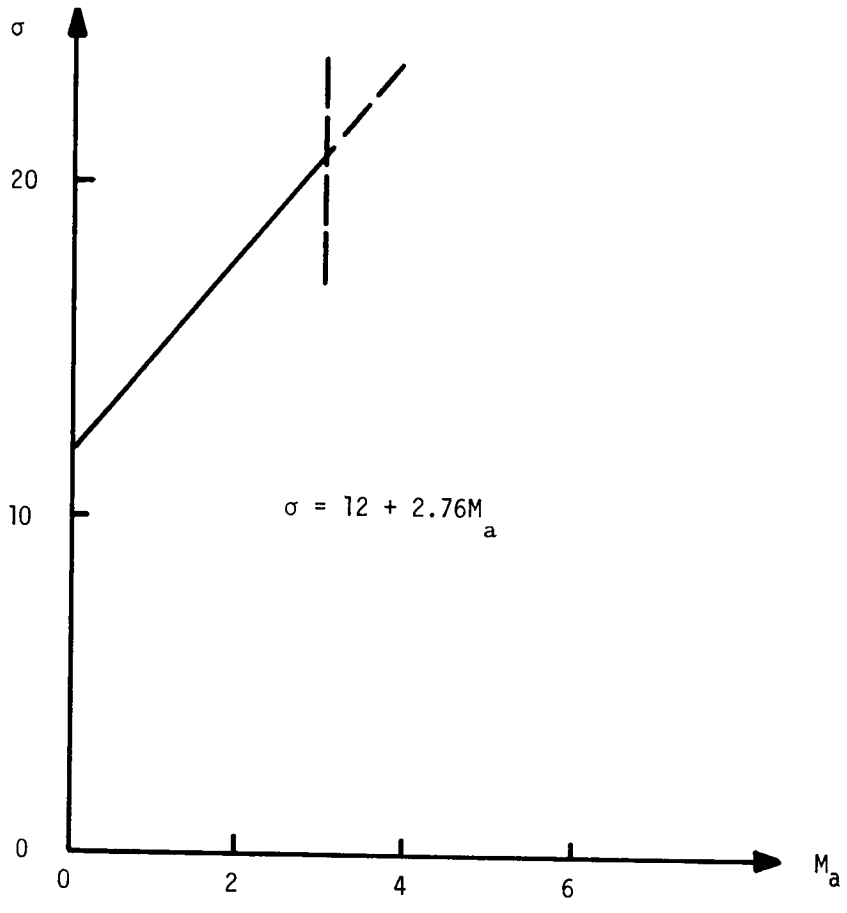

Figure 4.- Influence of free-stream Mach number on similarity parameter σ.

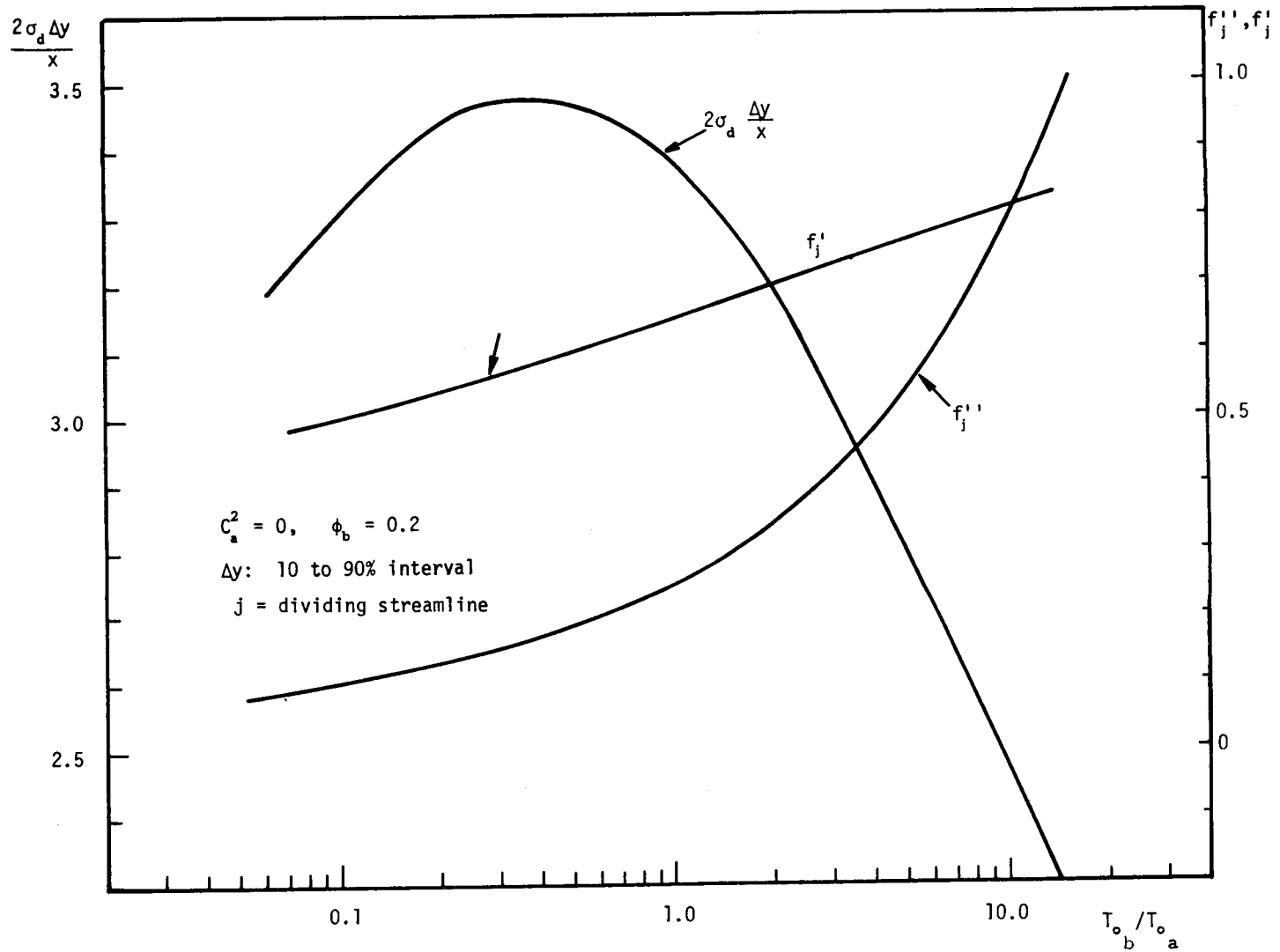

Figure 5.- Influence of density ratio (or temperature ratio) on similarity solution for two-stream mixing (d = 2).

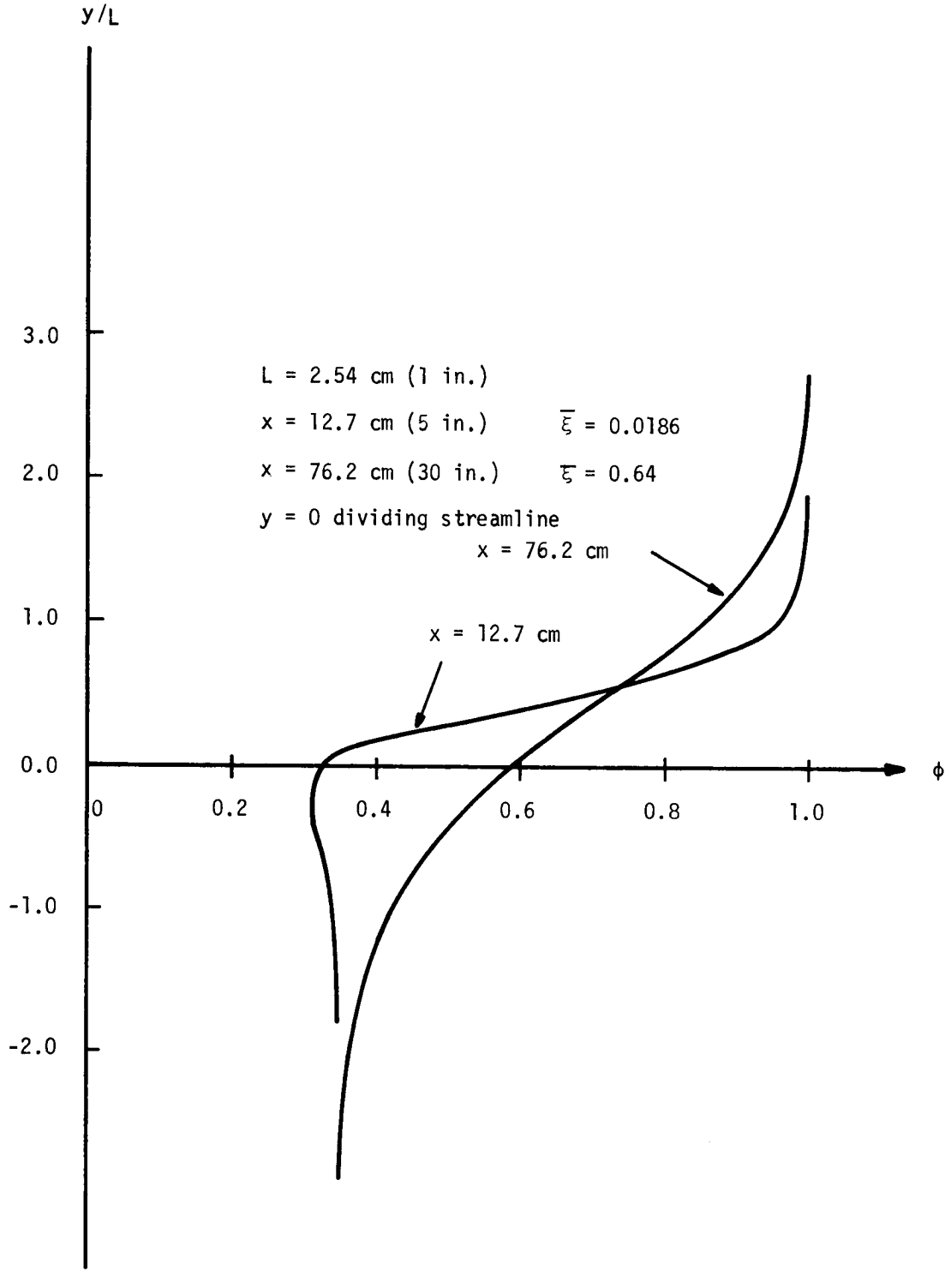

Figure 6.- Calculated velocity profiles at specified downstream locations for test case 4.

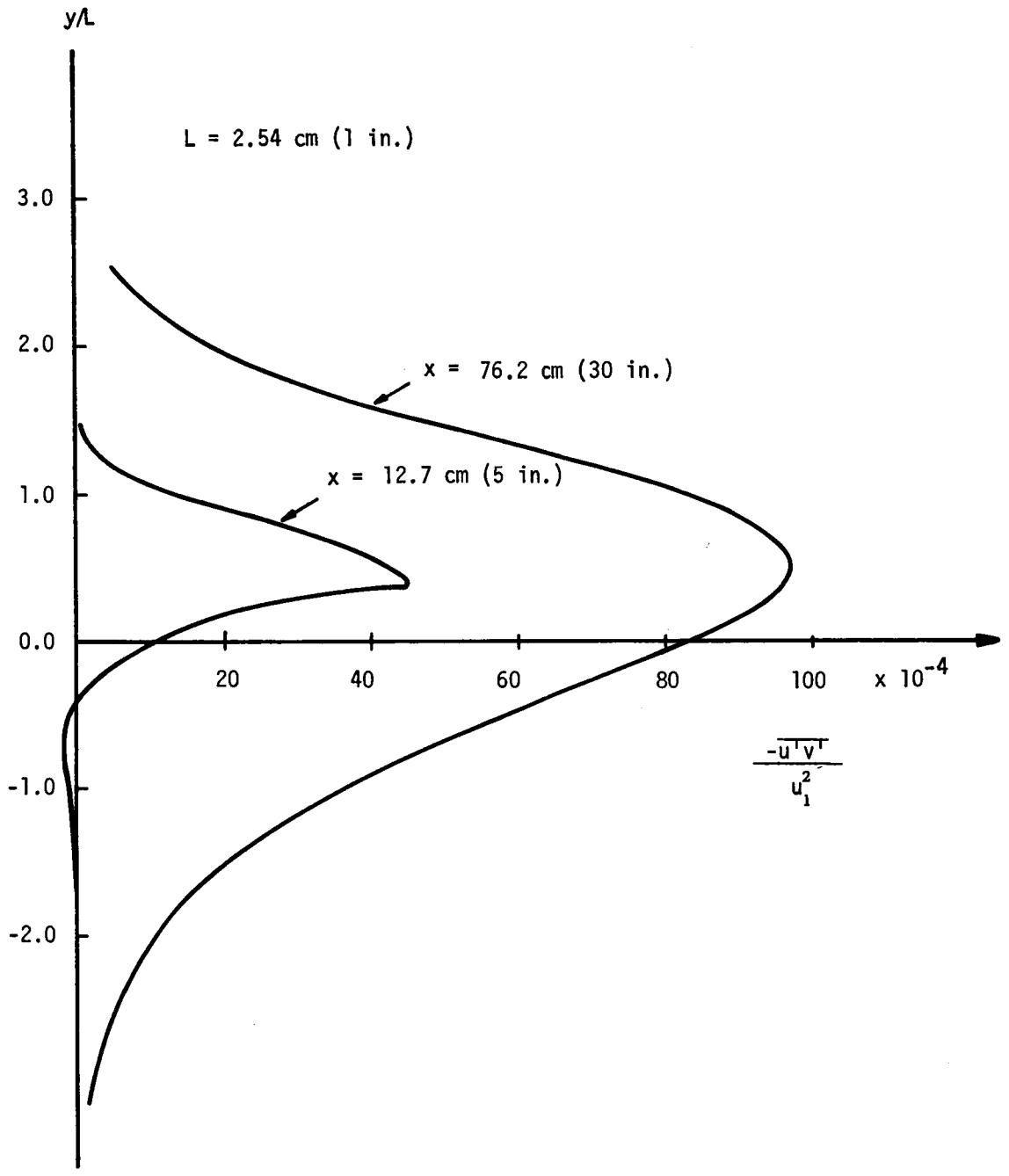

Figure 7.- Calculated shear stress profiles at specified downstream locations for test case 4.

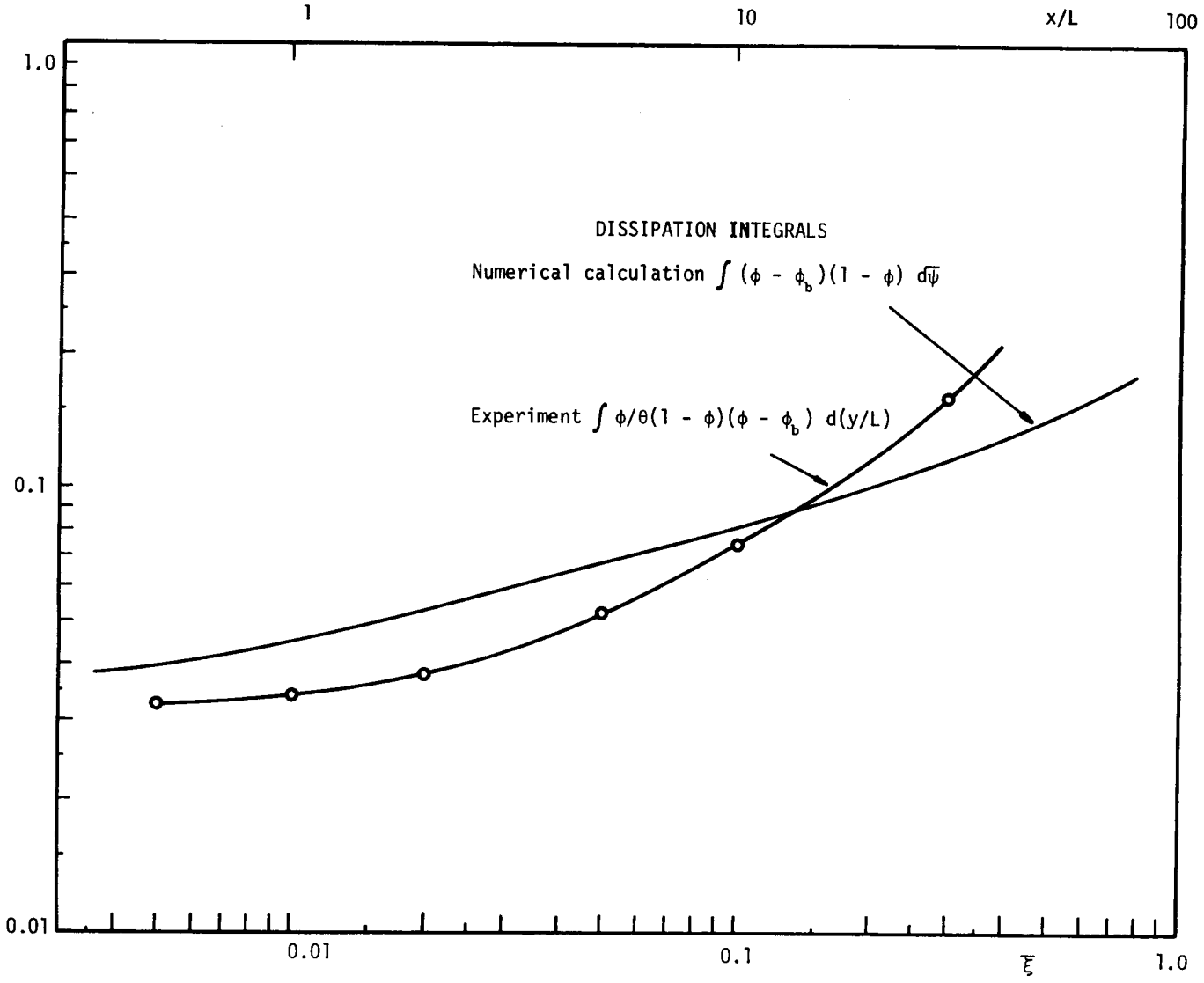

Figure 8.- Dissipation integrals as obtained by theoretical calculations and from experimental data for test case 4.

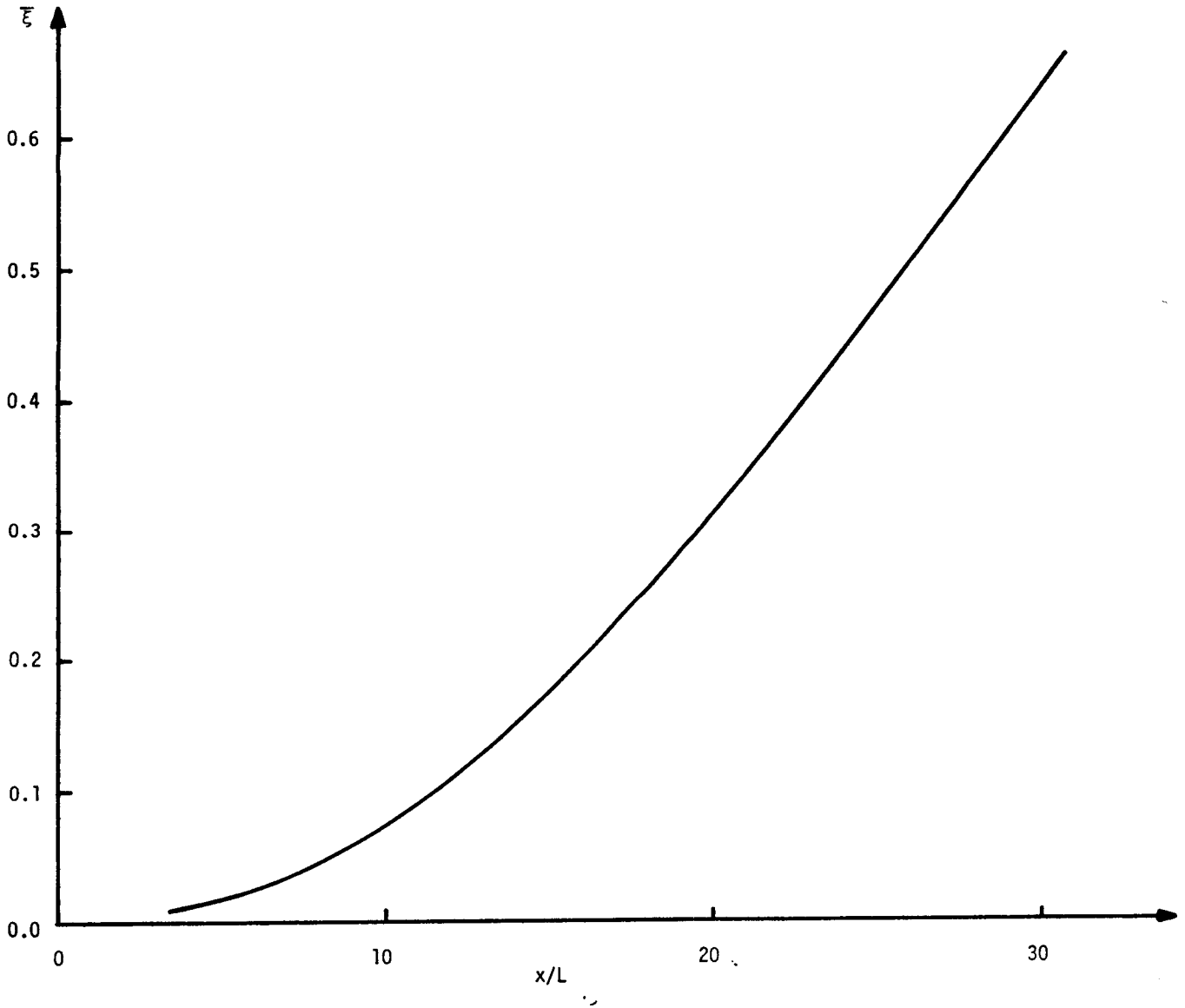

Figure 9.- Correlation of $\bar{\xi}$ and x/L by utilization of dissipation integrals for test case 4.

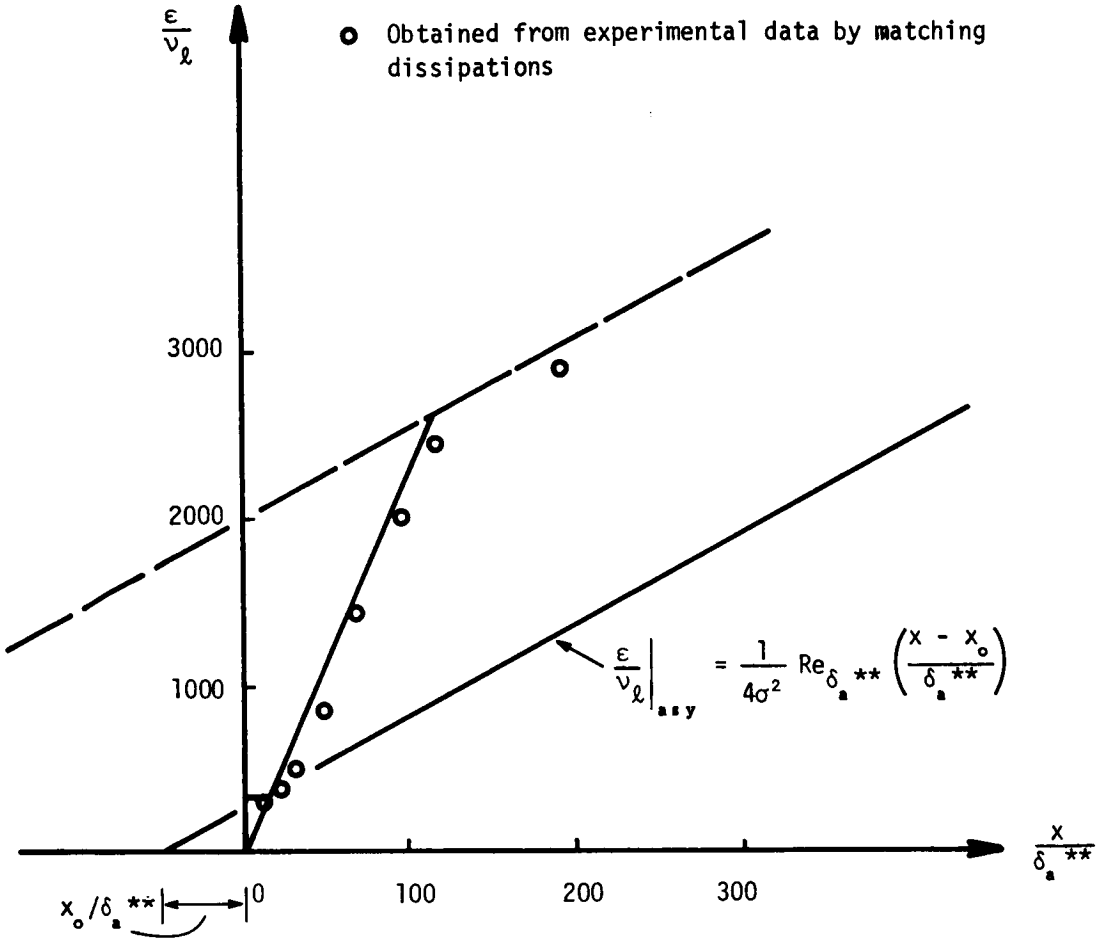

Figure 10.- Presentations of ϵ/ν for test case 4.

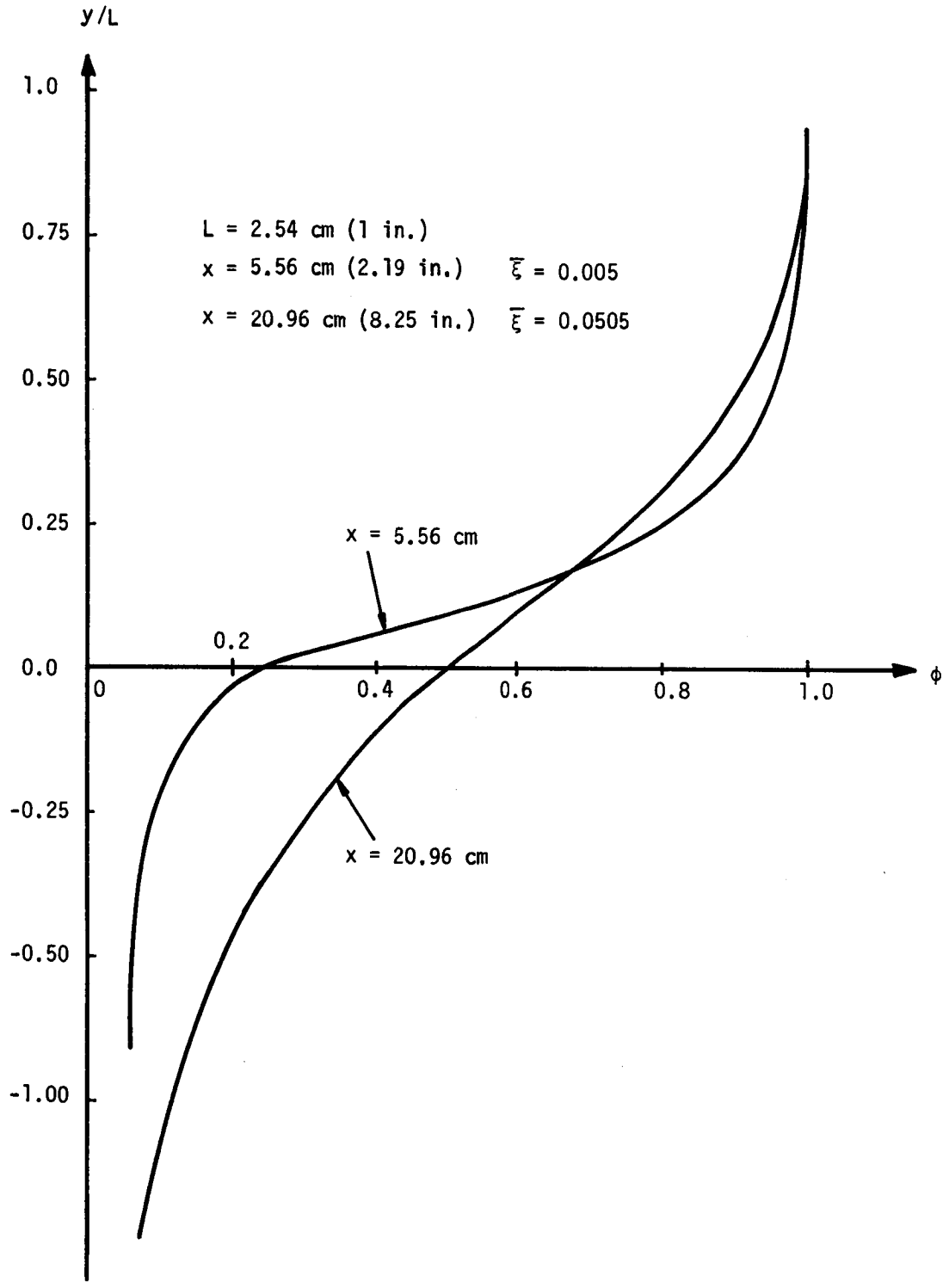

Figure 11.- Calculated velocity profiles at specified downstream locations for test case 5.

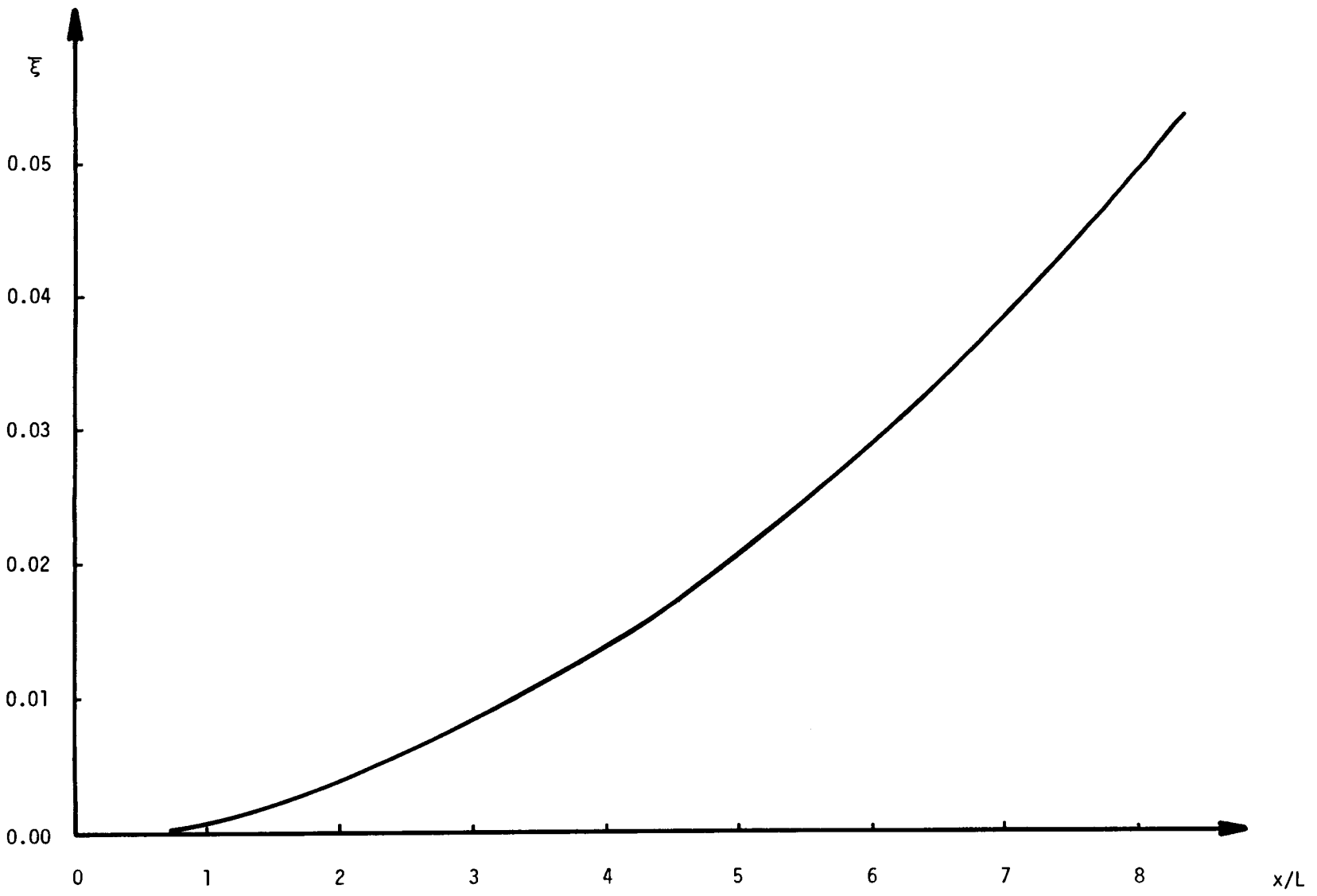

Figure 12.- Correlation of $\bar{\xi}$ and x/L by utilization of dissipation integrals for test case 5.

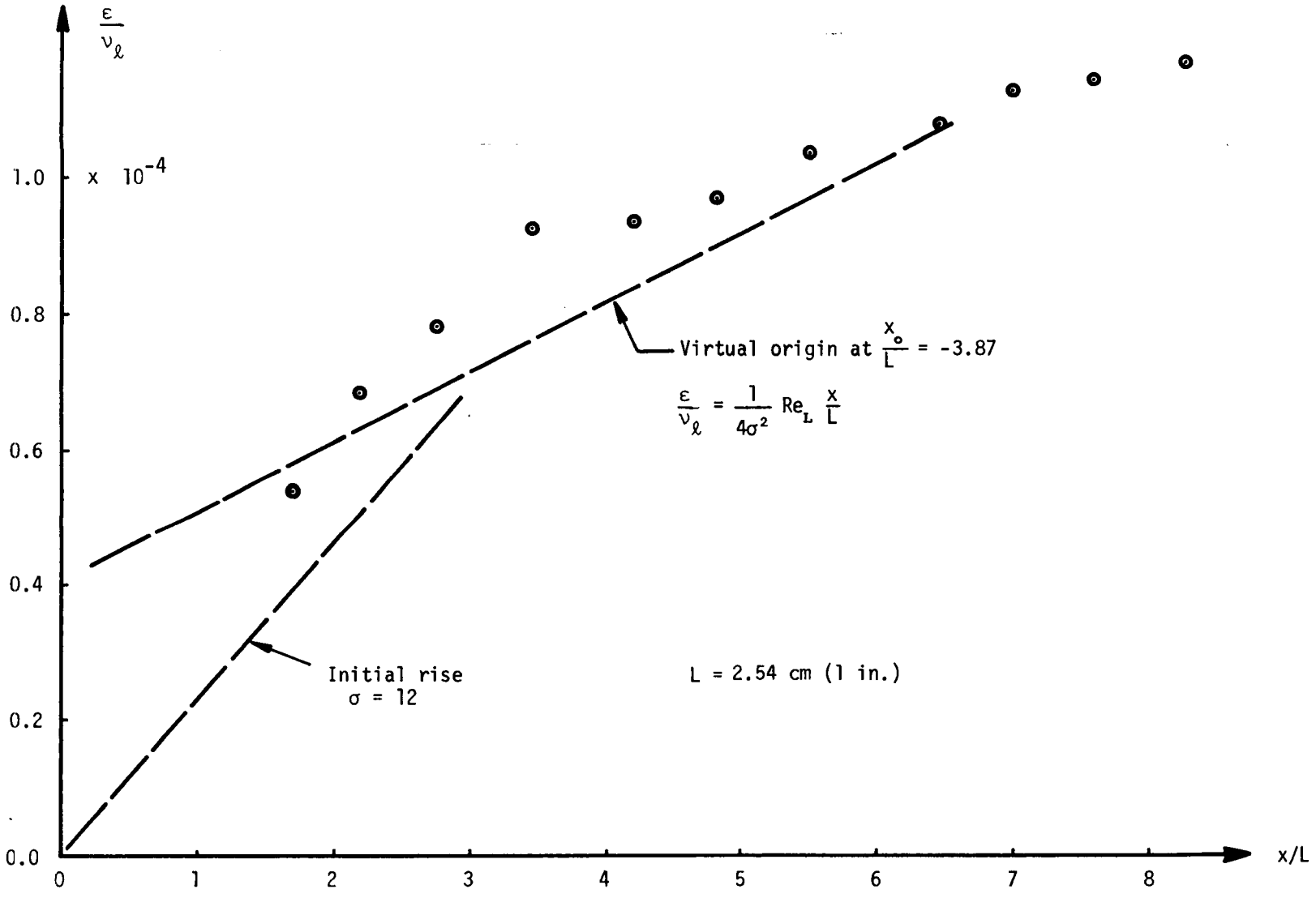

Figure 13.- Presentation of ϵ/ν for test case 5.

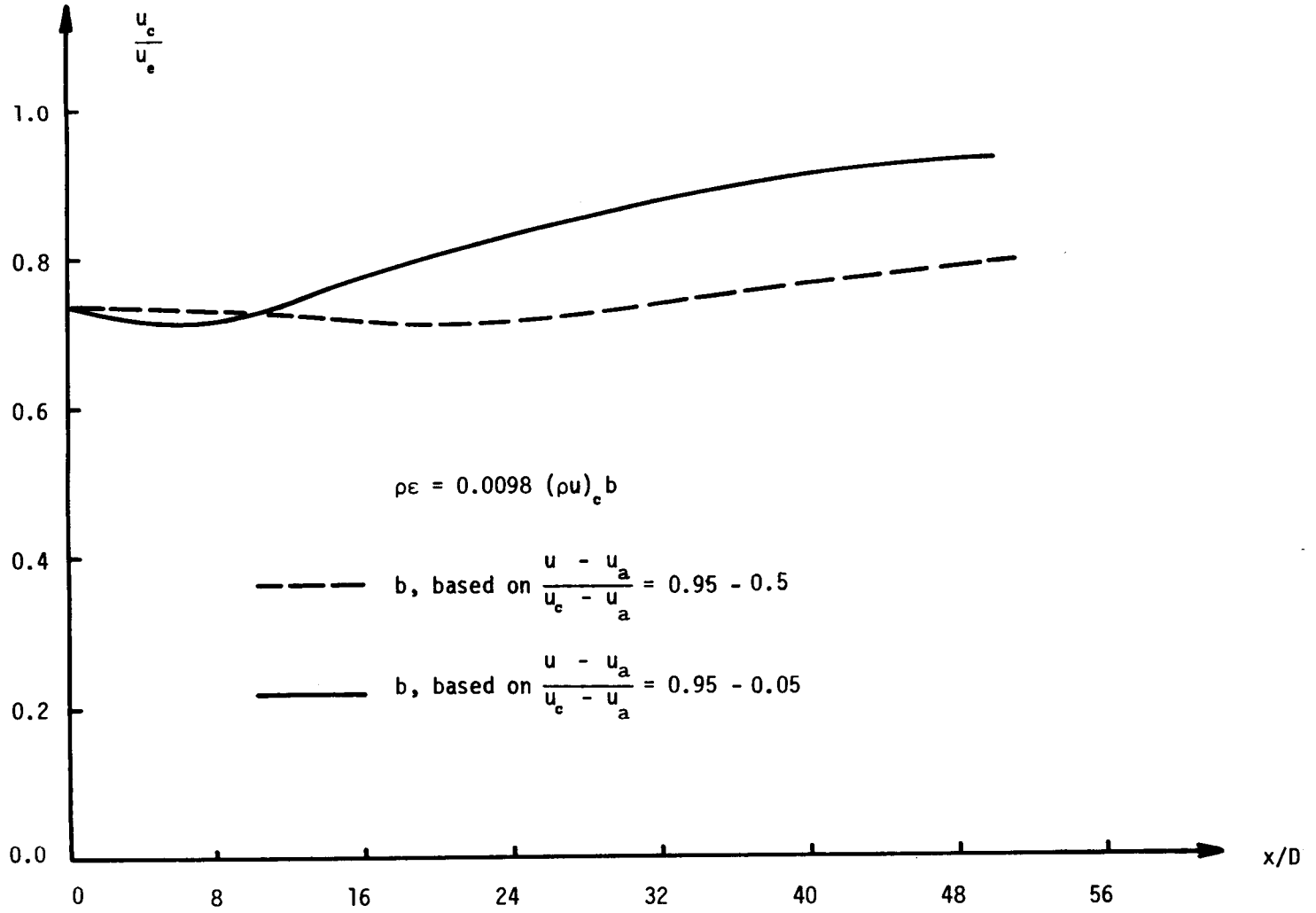

Figure 14.- Calculated center-line velocities for test case 11.

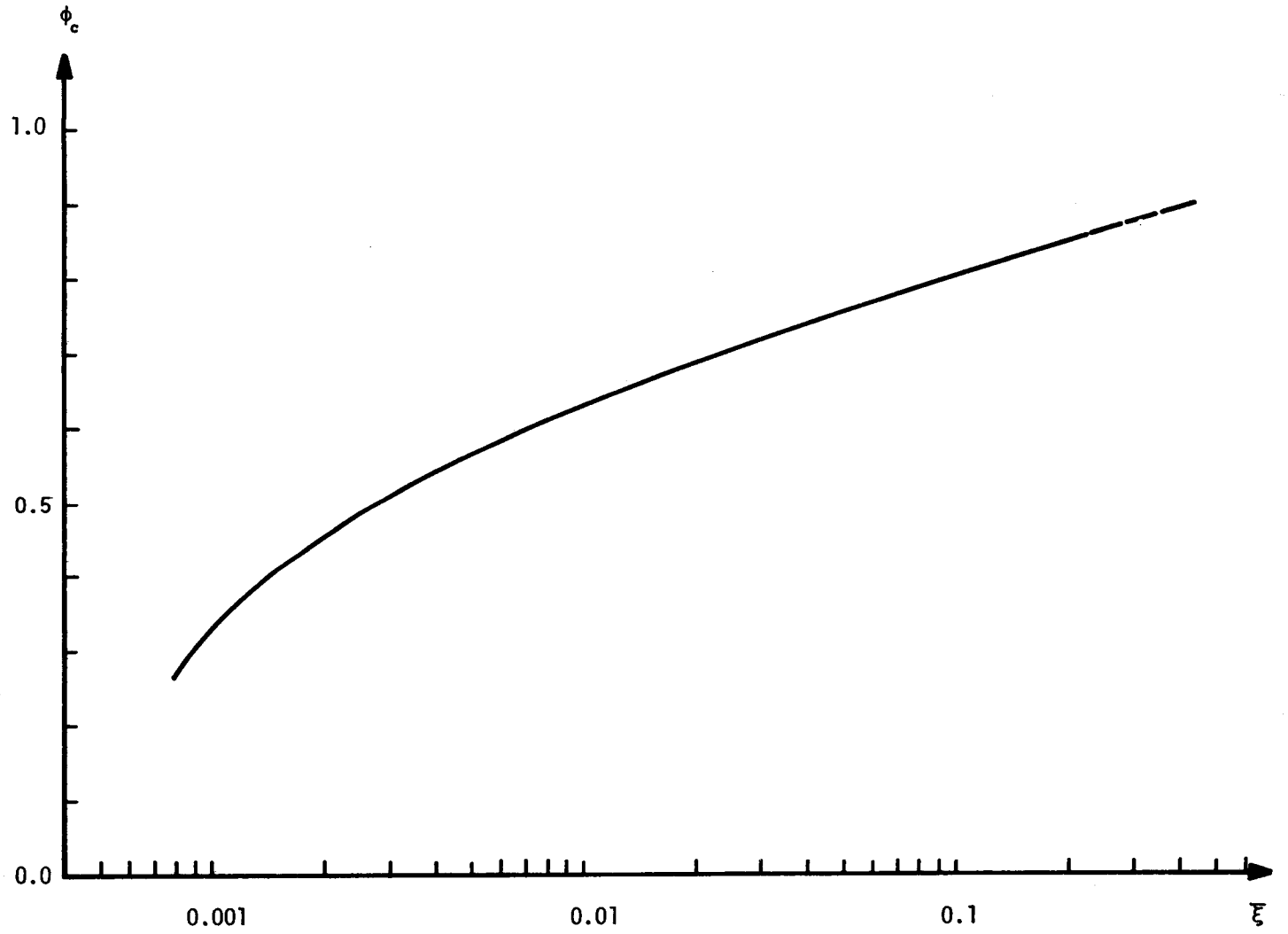

Figure 15.- Calculated center-line velocity as function of $\bar{\xi}$ for test case 14.

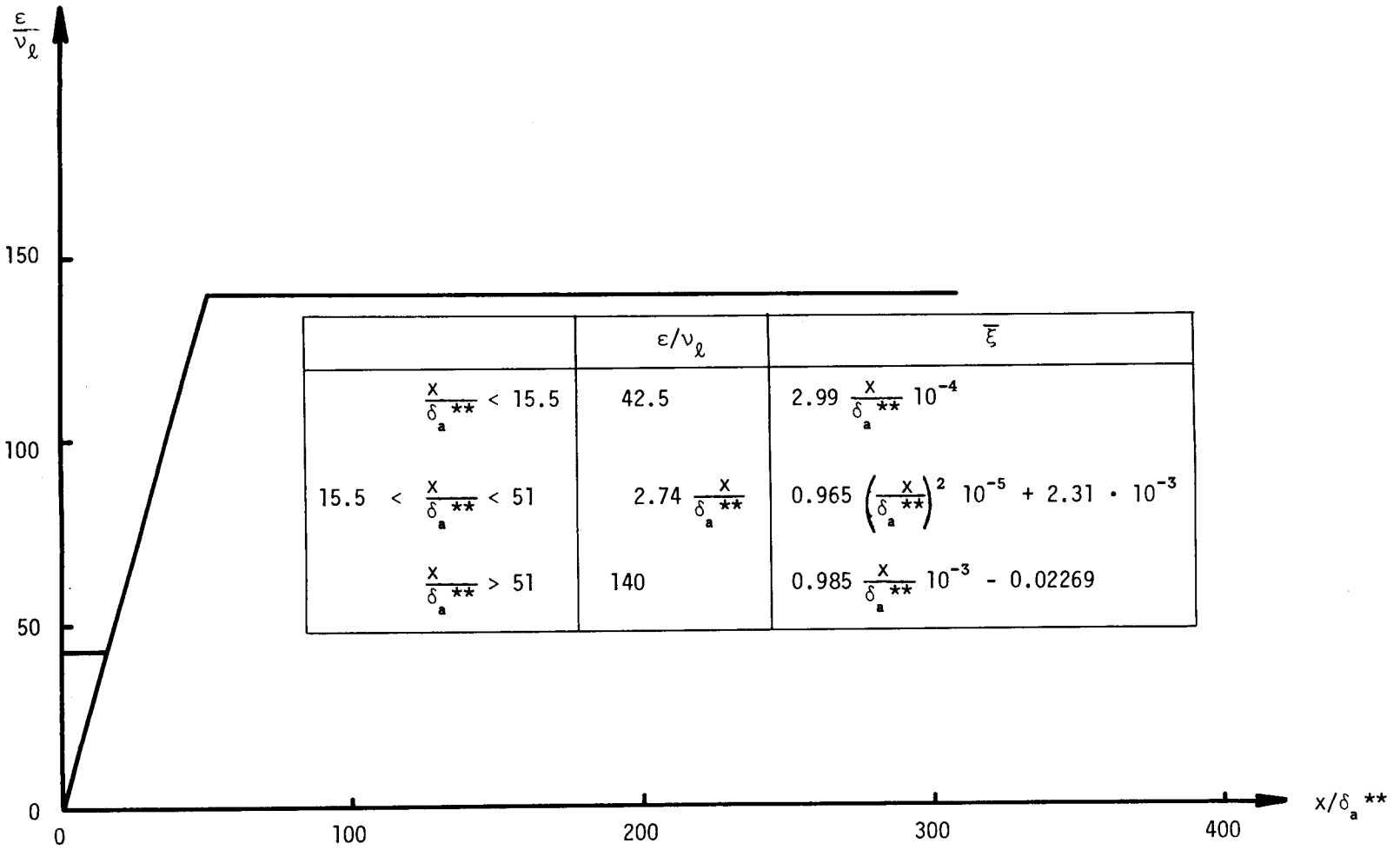

	ε/ν_ℓ	$\overline{\xi}$
$\frac{x}{\delta_a^{**}} < 15.5$	42.5	$2.99 \frac{x}{\delta_a^{**}} 10^{-4}$
$15.5 < \frac{x}{\delta_a^{**}} < 51$	$2.74 \frac{x}{\delta_a^{**}}$	$0.965 \left(\frac{x}{\delta_a^{**}}\right)^2 10^{-5} + 2.31 \cdot 10^{-3}$
$\frac{x}{\delta_a^{**}} > 51$	140	$0.985 \frac{x}{\delta_a^{**}} 10^{-3} - 0.02269$

Figure 16.- Viscosity model for test case 14.

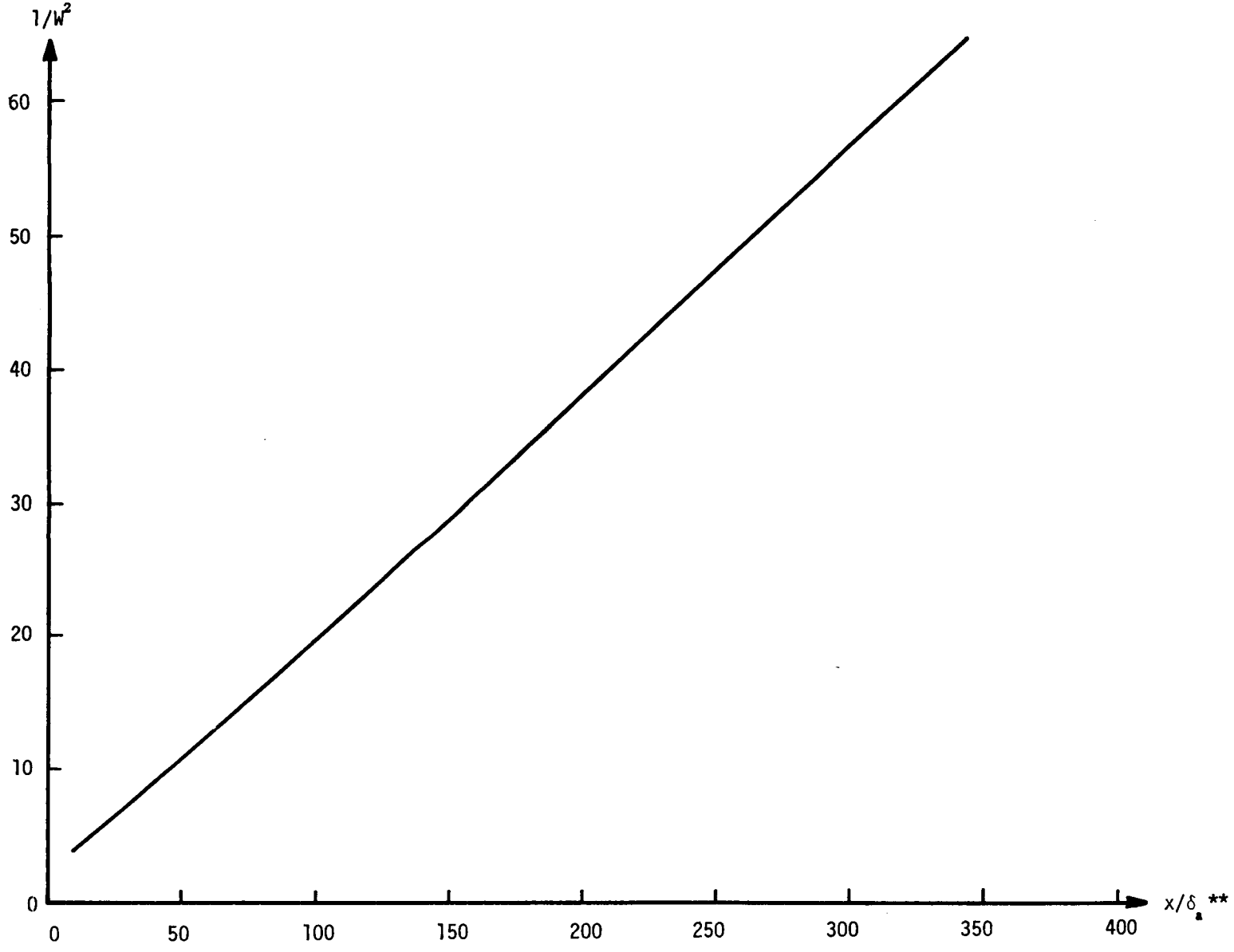

Figure 17.- Predicted center-line velocity defect for test case 14.

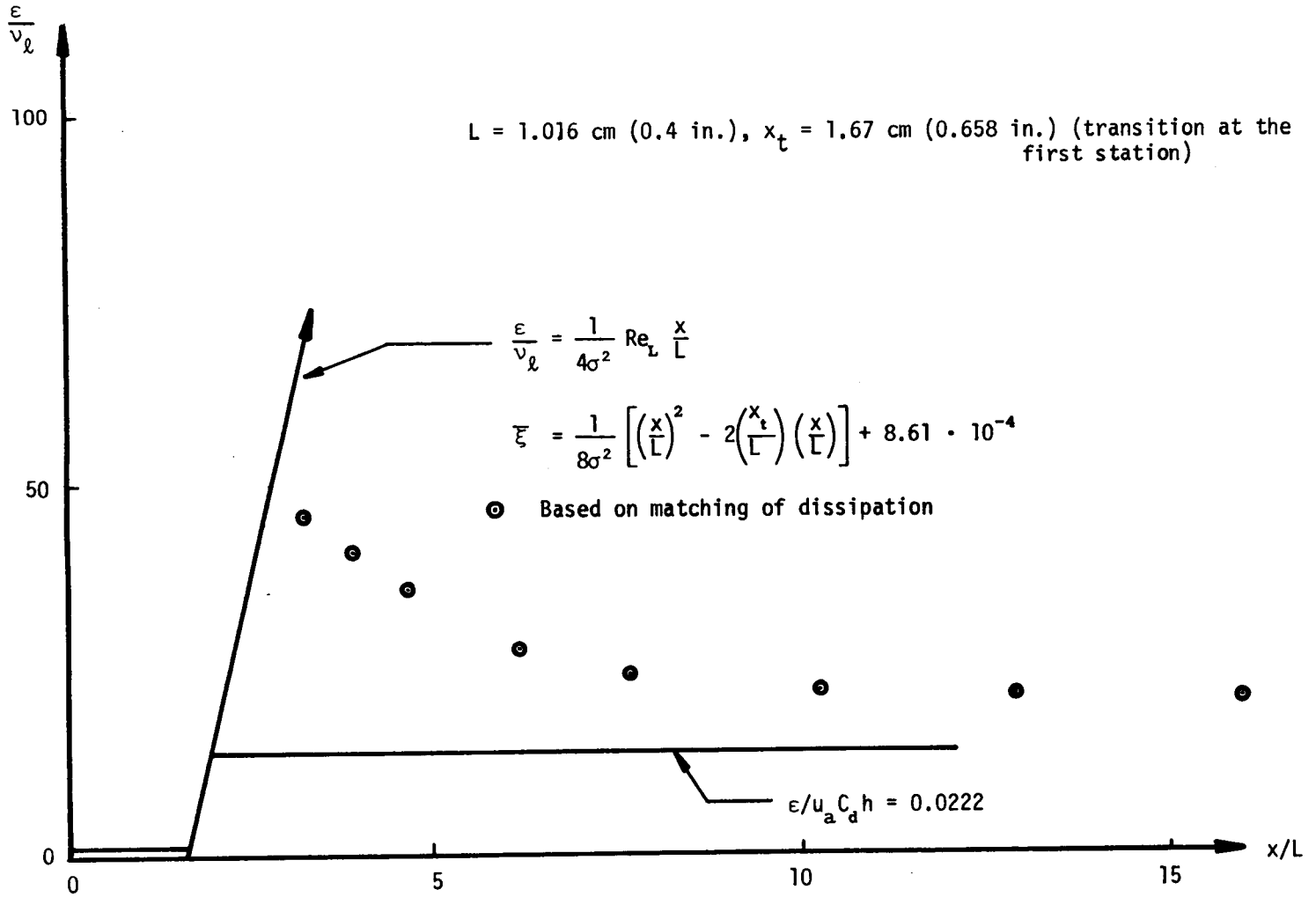

Figure 18.- Conceptual and experimentally determined eddy viscosity for test case 16.

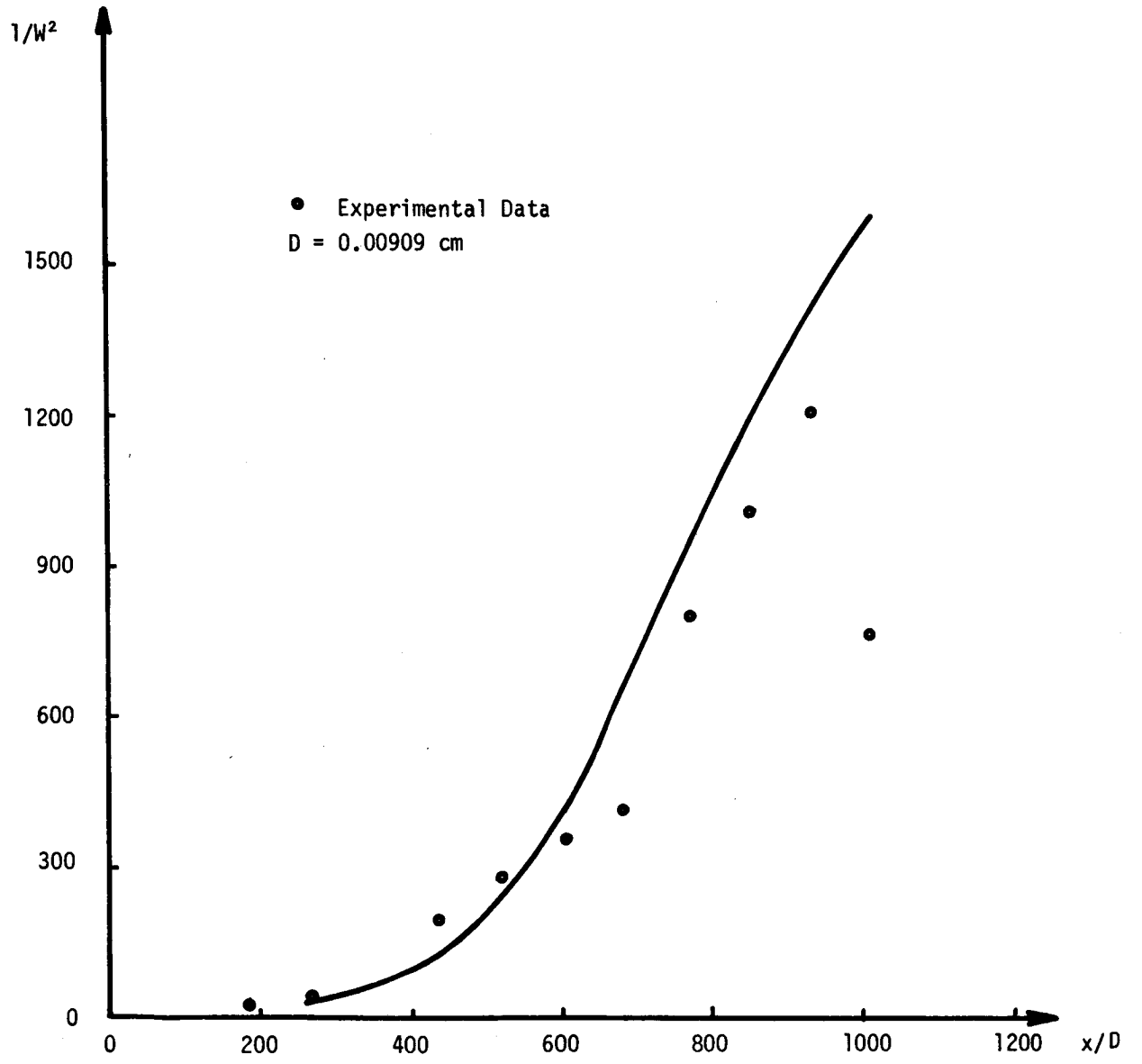

Figure 19.- Predicted and experimental center-line velocity defect for test case 16.

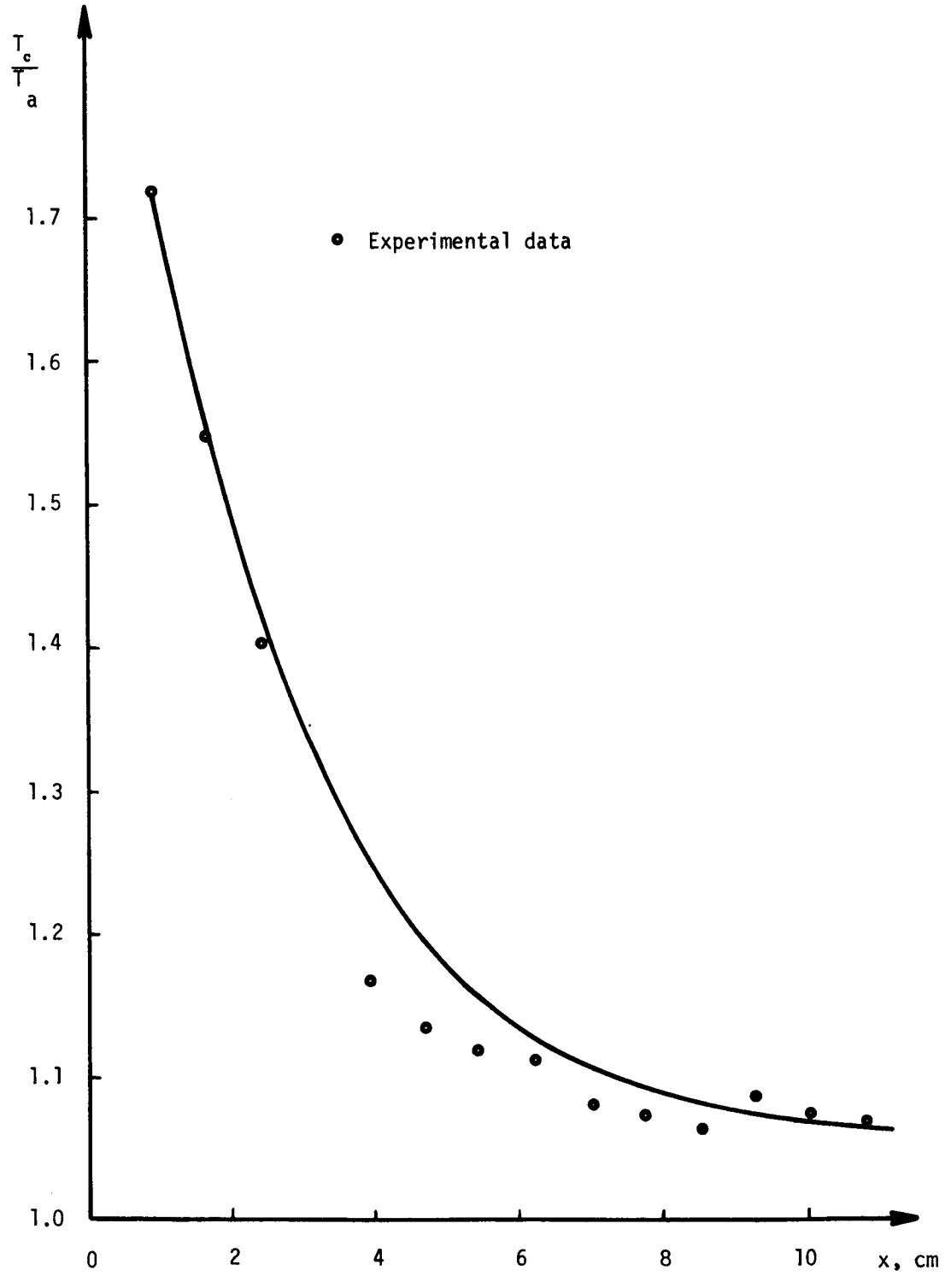

Figure 20.- Predicted and experimental center-line temperature ratio for test case 16.

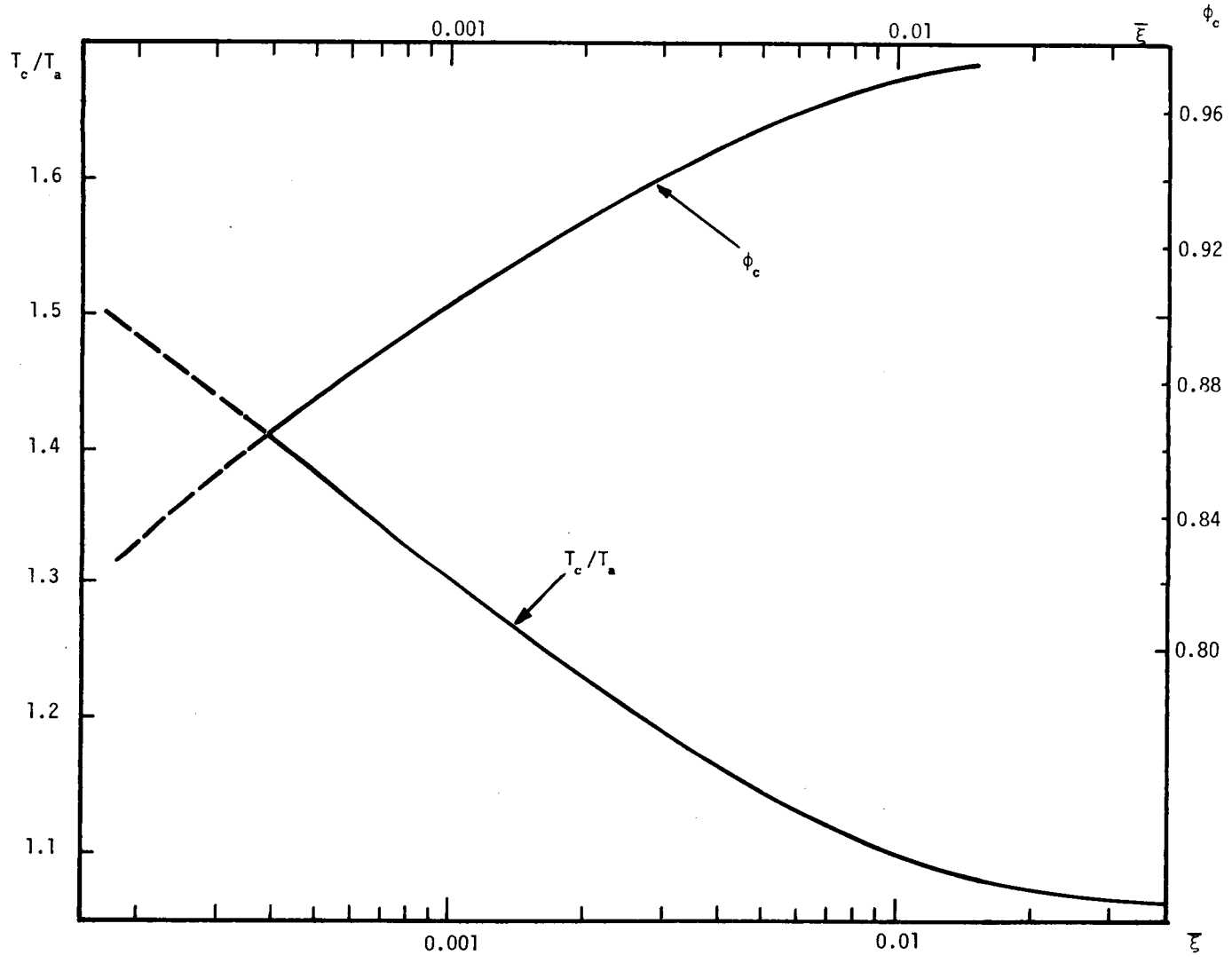

Figure 21.- Calculated center-line velocity and temperature ratios as functions of $\bar{\xi}$ for test case 16.

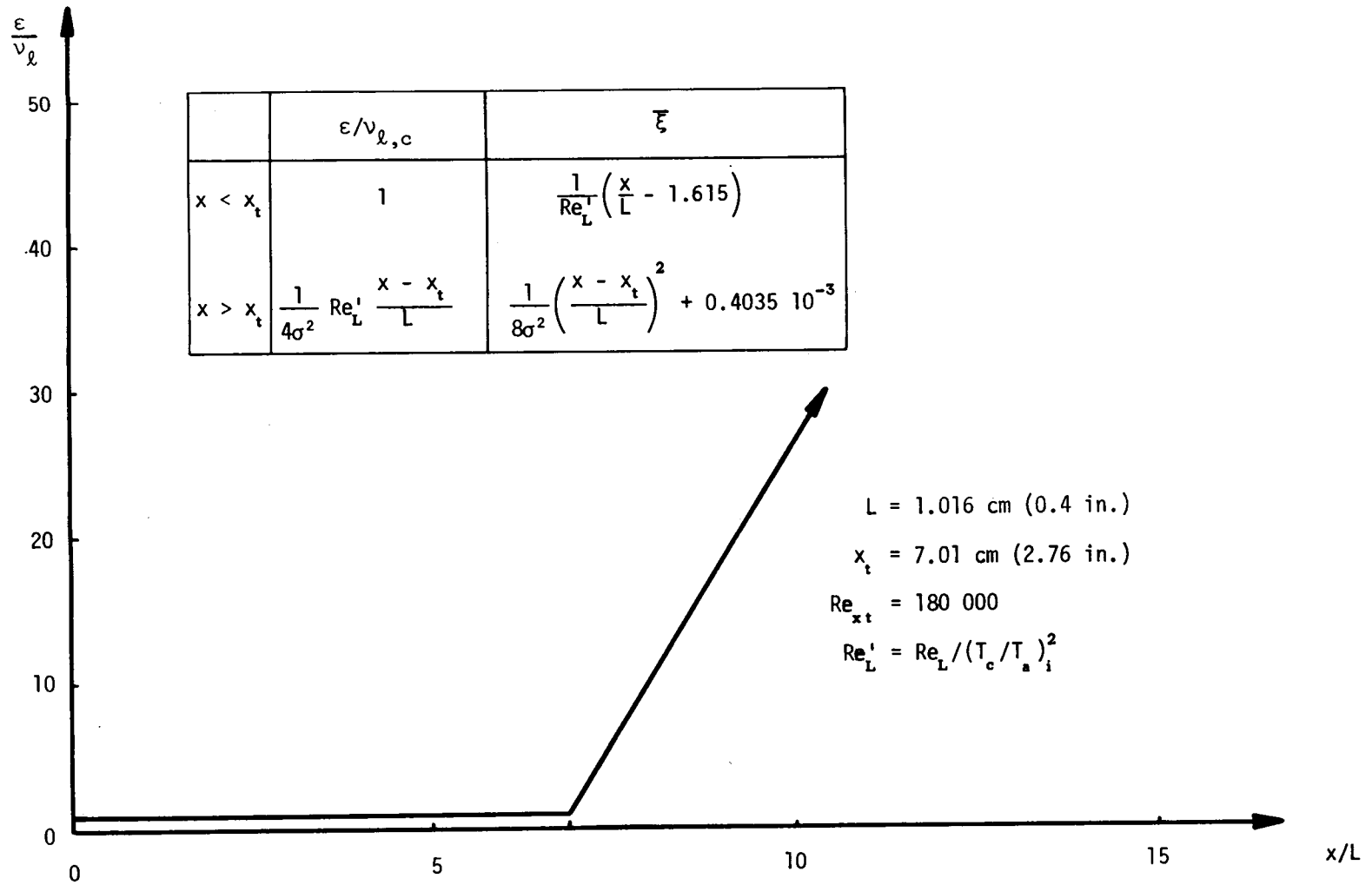

Figure 22.- Conceptual eddy viscosity for test case 24.

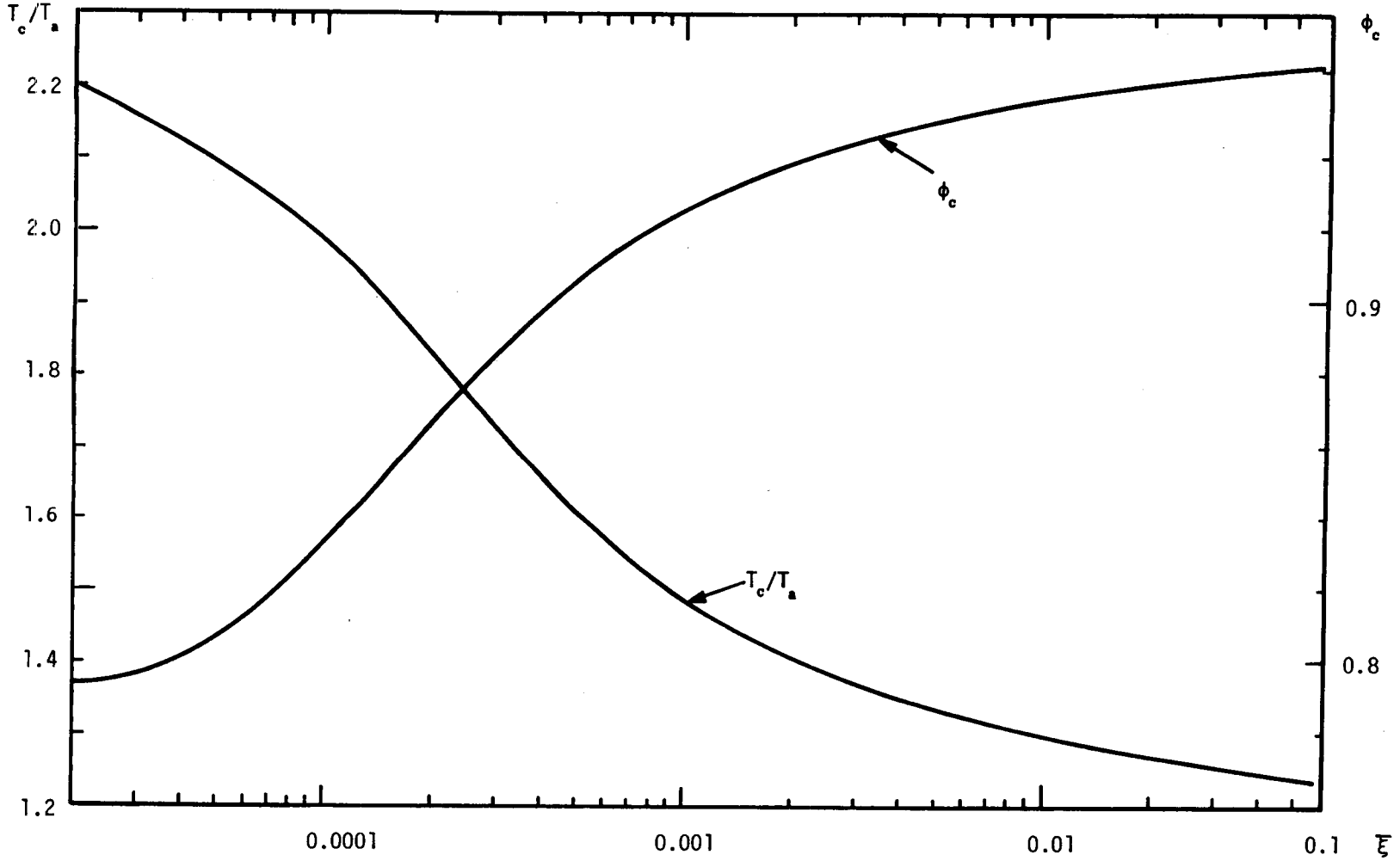

Figure 23.- Calculated center-line velocity and temperature ratios as functions of $\bar{\xi}$ for test case 24.

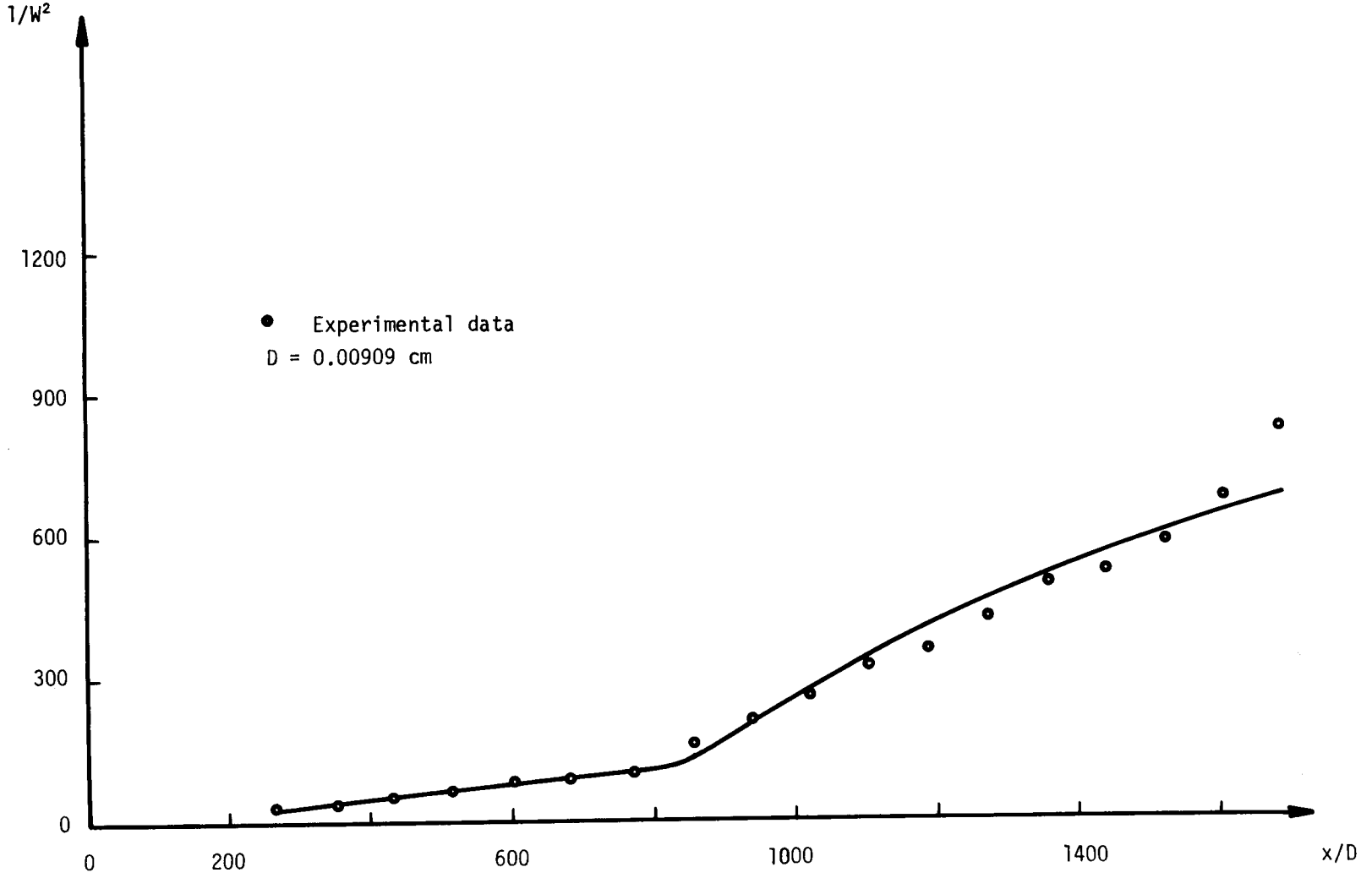

Figure 24.- Predicted and experimental center-line velocity defect for test case 24.

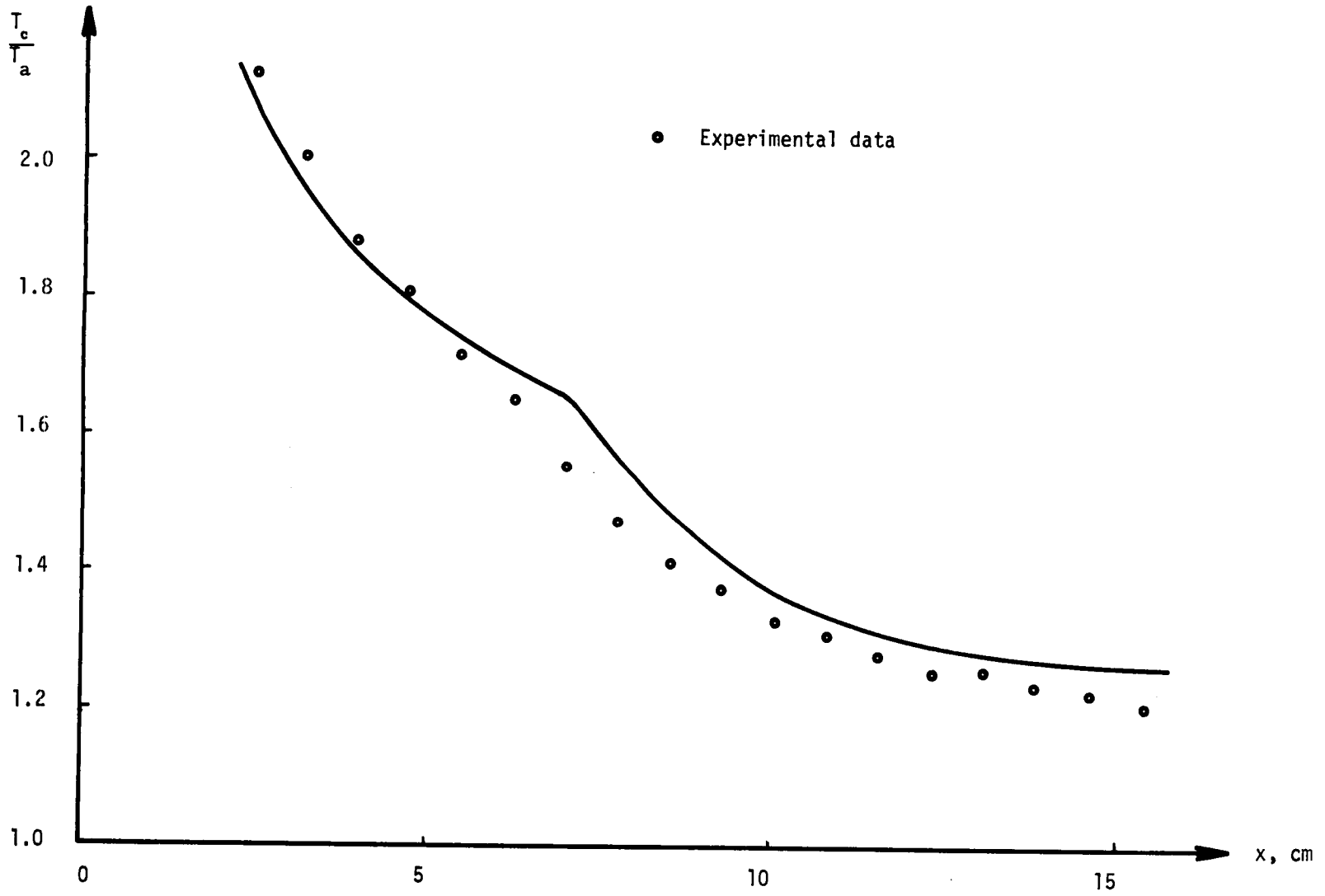

Figure 25.- Predicted and experimental center-line temperature ratios for test case 24.

Professor Goldschmidt: I am sorry, I must not have understood very well. How did you define your shift in the origin – this x_o – is it completely arbitrary or is it computed somehow?

W. L. Chow: No, first I said it is a matching of energy defect of the mean flow of the actual mixing profile to a fictitious one with a shifted origin, and meanwhile we have to also apply an equivalent bleed concept. In other words, if we have an initial boundary-layer flow, we always have a developing flow even far downstream. The flow looks similar, still shifted somewhat, so we have to use the initial boundary-layer effect to correlate it and we call that an equivalent bleed concept. It is described in the paper and it is long so I would rather not go into it at this time. If you would like to discuss anything else I would be glad to answer your question in detail, in private.